6040 J. Med. Chem. 2010, 53, 6040–6053
DOI: 10.1021/jm100432w

Journal of Medicinal Chemistry Article

Improved Syntheses of 5′-*S*-(2-Aminoethyl)-6-*N*-(4-nitrobenzyl)-5′-thioadenosine (SAENTA), Analogues, and Fluorescent Probe Conjugates: Analysis of Cell-Surface Human Equilibrative Nucleoside Transporter 1 (hENT1) Levels for Prediction of the Antitumor Efficacy of Gemcitabine

Morris J. Robins,*[,†] Yunshan Peng,[†,§] Vijaya L. Damaraju,[‡,§] Delores Mowles,[‡] Geraldine Barron,[‡] Tracey Tackaberry,[‡] James D. Young,[‡] and Carol E. Cass*[,‡]

[†]*Department of Chemistry and Biochemistry, Brigham Young University, Provo, Utah 84602-5700, and* [‡]*Departments of Oncology and Physiology, University of Alberta, Edmonton, Alberta, Canada T6G 1Z2.* [§]*These two authors were the major contributors for the chemistry (Y.P.) and nucleoside transport (V.L.D.) components of this paper.*

Received April 8, 2010

5′-*S*-(2-Aminoethyl)-6-*N*-(4-nitrobenzyl)-5′-thioadenosine (SAENTA), 5′-*S*-(2-acetamidoethyl)-6-*N*-[(4-substituted)benzyl]-5′-thioadenosine analogues, 5′-*S*-[2-(6-aminohexanamido)]ethyl-6-*N*-(4-nitrobenzyl)-5′-thioadenosine (SAHENTA), and related compounds were synthesized by S_NAr displacement of fluoride from 6-fluoropurine intermediates with 4-(substituted)benzylamines. Conjugation of the pendant amino groups of SAENTA and SAHENTA with fluorescein-5-yl isothiocyanate (FITC) gave fluorescent probes that bound at nanomolar concentrations specifically to human equilibrative nucleoside transporter 1 (hENT1) produced in recombinant form in model expression systems and in native form in cancer cell lines. Transporter binding effects were studied and the ability of the probes to predict the potential antitumor efficacy of 2′-deoxy-2′,2′-difluorocytidine (gemcitabine) was demonstrated.

Introduction

Specialized transmembrane proteins facilitate entry of nucleosides (including anticancer and antiviral drug analogues) into cells.[1−3] Seven such proteins in mammalian cells are presently categorized into two types of equilibrative (facilitative diffusion) and concentrative (active transport) nucleoside transporters (ENTs[a] and CNTs). ENTs mediate transport of nucleosides bidirectionally and most are driven by concentration gradients. CNTs transport nucleosides into cells actively, driven by Na^+ (and sometimes H^+) gradients. ENTs are more widely distributed in mammalian tissues than CNTs, which are found in epithelial cells and other specialized tissues. Two groups of ENT proteins are differentiated by their relative sensitivities to 6-*S*-(4-nitrobenzyl)-6-thioinosine (*p*-nitrobenzylmercaptopurine riboside: NBMPR) (**1**) (Chart 1). In humans and mice, ENT1s promote transport processes that are highly sensitive to inhibition by NBMPR (k_i = 0.1−1 nM). In contrast, ENT2s promote transport processes that are insensitive to inhibition by concentrations of NBMPR less than ∼1 μM. In human cells and tissues, hENT1 is the predominant nucleoside transporter.

There is increasing evidence that nucleoside transporters may serve as biomarkers for predicting response to nucleoside drugs.[4] Many studies have demonstrated the importance of hENT1 for cellular entry of nucleoside analogue drugs and manifestation of their toxicities.[5−9] More recently, studies with samples from patients with pancreatic cancer have revealed that hENT1-mediated nucleoside transport is an important determinant of responses to 2′-deoxy-2′,2′-difluorocytidine (gemcitabine) because patient response was positively correlated with the abundance of hENT1 protein in cancer tissues as measured by immunohistochemistry.[10−12] That method, which utilizes monoclonal antibodies directed against a synthetic peptide derived from hENT1,[13] is applicable to paraffin-embedded or frozen tissue samples but is time-consuming (cell fixation, permeabilization, and antigen retrieval are required) and therefore less useful for routine monitoring of site densities with freshly isolated cells. Enumeration of nucleoside-transport sites on such cells can be performed by equilibrium binding of [^{3}H]NBMPR, but this method cannot distinguish among subpopulations of cells with different transporter densities or between internal and cell-surface transporter molecules. A high-affinity fluorescent analogue that can be used to determine cell-surface abundances of hENT1 enables rapid quantification of hENT1 sites

*To whom correspondence should be addressed. For chemistry (M.J.R.): phone, (801) 422-6272; fax, (801) 422-0153; E-mail, morris_robins@byu.edu. For nucleoside transport (C.E.C.): phone, (780) 432-8509; fax, (780) 432-8886; E-mail: carolcass@albertahealthservices.ca.

[a]Abbreviations: AcSAENTA, 5′-*S*-(2-acetamidoethyl)-6-*N*-(4-nitrobenzyl)-5′-thioadenosine; CNT, concentrative nucleoside transporter; ENT, equilibrative nucleoside transporter; FITC, fluorescein-5-yl isothiocyanate; FITC-SAENTA, 5′-*S*-{2-[3-(fluorescein-5-yl)thioureido-1-yl]}ethyl-6-*N*-(4-nitrobenzyl)-5′-thioadenosine; FITC-SAEPTA, 5′-*S*-{2-[3-(fluorescein-5-yl)-thioureido-1-yl]}ethyl-6-*N*-[4-(propanamido)benzyl]-5′-thioadenosine; FITC-SAHENTA, 5′-*S*-{2-(6-[3-(fluorescein-5-yl)thioureido-1-yl]hexanamido)}ethyl-6-*N*-(4-nitrobenzyl)-5′-thioadenosine; FITC-SAHEPTA, 5′-*S*-{2-(6-[3-(fluorescein-5-yl)thioureido-1-yl]hexanamido)}ethyl-6-*N*-[4-(propanamido)benzyl]-5′-thioadenosine; hENT1, human equilibrative nucleoside transporter 1; MESF, molecules of equivalent soluble fluorescein; MTS, 3-(4,5-dimethylthiazol-2-yl)-5-(3-carboxymethoxyphenyl)-2-(4-sulfophenyl)-2*H*-tetrazolium; NBAdo, 6-*N*-(4-nitrobenzyl)-adenosine; NBMPR, *p*-nitrobenzylmercaptopurine riboside [6-*S*-(4-nitrobenzyl)-6-thioinosine]; SAENTA, 5′-*S*-(2-aminoethyl)-6-*N*-(4-nitrobenzyl)-5′-thioadenosine; SAEPTA, 5′-*S*-(2-aminoethyl)-6-*N*-[4-(propanamido)benzyl]-5′-thioadenosine; SAHENTA, 5′-*S*-[2-(6-aminohexanamido)]ethyl-6-*N*-(4-nitrobenzyl)-5′-thioadenosine; SAHEPTA, 5′-*S*-[2-(6-aminohexanamido)]ethyl-6-*N*-[4-(propanamido)benzyl]-5′-thioadenosine.

 Published on Web 07/23/2010

Chart 1. Structures of Nucleoside Transport Inhibitors **1**−**7b**

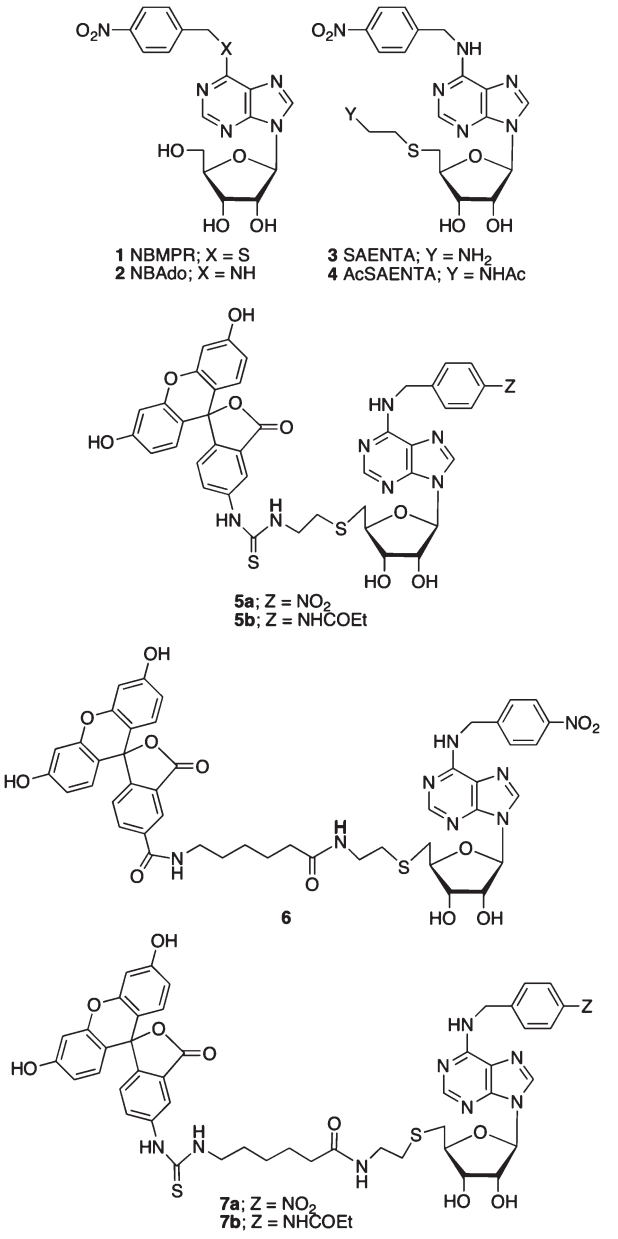

in clinical samples and allows predictions of treatment outcomes with nucleoside drugs.[14]

NBMPR (**1**), NBAdo (**2**), SAENTA (**3**), AcSAENTA (**4**), and FITC-SAENTA (**5a**) are bound tightly by hENT1. The fluorescent **5a**[15] was shown to be a high-affinity probe for hENT1 sites on cells by flow cytometry,[15−17] and quantification of hENT1 site densities on cultured cells and in freshly isolated clinical samples was demonstrated.[16,18,19] Alkylation of 6-thioinosine with 4-nitrobenzyl halides provided easy access to NBMPR,[20] but it is not an ideal biomedical agent because S_NAr displacement of 4-nitrobenzylthiolate from C6 of the purine ring by nucleophiles and homolytic cleavage of the benzyl−sulfur bond (promoted by UV light[21]) are possible. NBAdo and analogues are more chemically stable and also are bound tightly by ENT1s.[22−24] The 5′-*S*-(2-acetamidoethyl) derivative **4** was bound well by the transporter from pig erythrocyte ghosts, whereas replacement of the nitro substituent on the phenyl ring of **2** with carboxamido or sulfonamido groups produced analogues with much weaker binding affinities. Structure−activity relationship (SAR) studies showed that the 4-nitrobenzyl moiety on sulfur or nitrogen at C6 of the purine ring made a major contribution to binding. Structural modifications were well tolerated at the C5′ terminus, and conjugation of Affi-Gel 10 with the amino group on the 5′-substituent of **3** produced a support for affinity-chromatographic enrichment of the transporter protein.[22] Conjugation of fluorescein-5-yl isothiocyanate (FITC) with **3** gave the thioureido-linked probe **5a**[15] (FITC-SAENTA; also dubbed SAENTA-χ_2-fluorescein, where χ_2 indicated the number of atoms in the linkage between fluorescein and the aminoethyl nitrogen atom of **3**), and Jamieson et al.[16] noted that fluorescence output with their extended "5-(SAENTA-χ_8)-fluorescein" analogue **6** was higher than that with **5a**. Reliable samples of **5a** and **6** were not available, and the outlined synthesis of SAENTA[22] was problematic (poor overall yields of **3** often contaminated with byproducts).

We now report improved methods for the synthesis of **3**, **4** and modified acetamido analogues, **5a**, and the new conjugate **5b**. We also prepared the new analogues 5′-*S*-[2-(6-aminohexanamido)]ethyl-6-*N*-(4-nitrobenzyl)-5′-thioadenosine (SAHENTA), 5′-*S*-[2-(6-aminohexanamido)]ethyl-6-*N*-(4-propanamidobenzyl)-5′-thioadenosine (SAHEPTA), and their FITC conjugates **7a** and **7b** that have the linker between C5 of fluorescein and C5′ of the nucleoside moieties in **7a** and **7b** extended by seven atoms from that in **5a** and **5b**. We measured cell-surface staining of hENT1 sites in several cell types by fluorescence detection of the binding with **7a** at nanomolar levels. Cellular uptake of the anticancer drug gemcitabine was associated with the abundance of transporter populations at cell surfaces, which provides methodology for prediction of potential clinical efficacy.

Chemistry

Our prior studies with 6-*N*-(substituted)adenosine compounds revealed large differences in binding affinities for derivatives with different groups on N6 of adenine.[22−24] Significant variations in binding affinities were observed with modifications on the phenyl ring of 6-*N*-(substituted-benzyl)adenosines, whereas changes at the 5′-*S*-(2-aminoethyl) moiety were well tolerated. Therefore, we synthesized and evaluated 5′-*S*-(2-acetamidoethyl) analogues of **3** with various substituents at C6 of the purine moiety to identify promising candidates for conjugation with FITC.

The Agbanyo et al. synthesis of **3**[22] employed alkylation of the adenine moiety at N1 followed by Dimroth rearrangement to the N6 isomer. Those steps, and others in the sequence, produced byproducts that were difficult to separate and poor overall yields of contaminated **3** were often obtained. Our diazotization/fluorodediazoniation of aminopurine nucleosides[25,26] and S_NAr displacement of fluoride with amines[27] occurred under mild conditions that offered an attractive route for synthesis of the desired compounds. Selective acetylation of the hydroxyl groups of the model substrate 5′-chloro-5′-deoxyadenosine[28] (**8**) (Scheme 1) and treatment of the 2′,3′-di-*O*-acetyl derivative with $NaNO_2$ in ∼55% HF-pyridine at −25 to 0 °C produced the 6-fluoropurine compound **9** (86%) without incident. Solid $NaNO_2$ was more convenient and safer than *tert*-butyl nitrite,[25] but the HF-pyridine concentration and temperature conditions were more demanding.

Treatment of **8** with the sodium thiolate generated from 2-acetamidoethanethiol gave 5′-*S*-(2-acetamidoethyl)-5′-deoxy-5′-thioadenosine (**10**). The 2′,3′-di-*O*-acetyl derivative

Scheme 1. Synthesis of 6-Fluoropurine Intermediate **11a**[a]

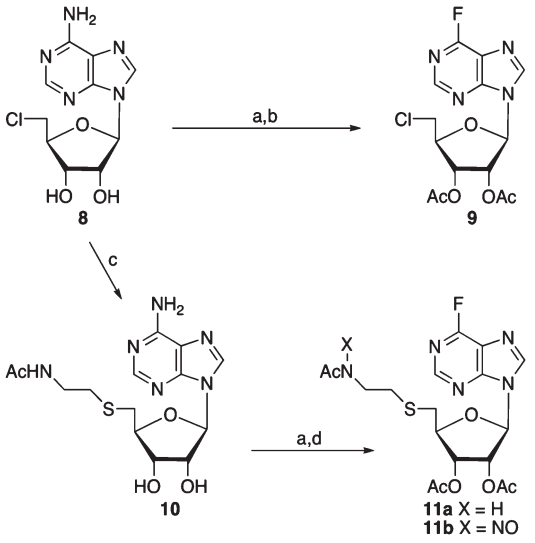

[a] Reagents and conditions: (a) Ac_2O, pyridine, 0 °C; (b) $NaNO_2$, ~55% HF-pyridine, −25 to 0 °C; (c) $AcNH(CH_2)_2SH$, NaH, DMF, 70 °C; (d) $NaNO_2$, ~55% HF-pyridine, −10 to −5 °C.

was prepared readily, but diazotization/fluorodediazoniation did not proceed as cleanly. Lower temperatures and/or equivalent ratios of $NaNO_2$ resulted in slower formation of the desired 6-fluoropurine product and generation of more decomposition byproducts. Higher temperatures or ratios of $NaNO_2$ produced increased quantities of an *N*-nitrosoamide byproduct. For example, $NaNO_2$ (6.5 equiv) in HF-pyridine (~55%) at −10 to −5 °C gave 9-[5-*S*-(2-acetamidoethyl)-2,3-di-*O*-acetyl-5-deoxy-5-thio-β-D-ribofuranosyl]-6-fluoropurine (**11a**) (28%) plus **11b** (56%), whereas 1.5 equiv of $NaNO_2$ under the same conditions gave **11a** (64%) plus **11b** (24%). Clean **11a** for the preparation of the model binding probes was obtained by flash chromatography.

Nucleoside binding affinity for hENT1 is enhanced by a 4-nitrobenzyl group at N6 (or S6) of the purine moiety,[20,23] but nitro groups can participate in single electron transfer (SET) reactions and activate systems for photochemical processes.[21] Therefore, we also evaluated amide analogues linked through the carbonyl carbon or amide nitrogen at C4 of the appended benzyl rings. Trifluoroacetylation of 4-(aminomethyl)benzoic acid (**12**) (Scheme 2), treatment of the trifluoroacetamido intermediate with thionyl chloride, and addition of an amine gave the 4-[(trifluoroacetamido)methyl]benzamides **13**, which were purified before removal of the trifluoroacetyl group to give the 4-(aminomethyl)benzamides **14**. Treatment of 4-{[(*tert*-butyloxycarbonyl)amino]methyl}aniline (**15**) with acyl or sulfonyl chlorides gave the 4-[(Boc-amino)methyl]-*N*-(acyl or sulfonyl)anilines **16** that were deprotected to give the 4-(aminomethyl)-*N*-(acyl or sulfonyl)anilines **17**.

Compound **11a** underwent clean and rapid S_NAr displacement of fluoride[27] with the 4-substituted benzylamines **14a**−**14j** and **17k**−**17t** in MeOH at ambient temperature. Deacetylation of the intermediates (only the intermediate diacetate from **17k** was purified and characterized) gave the model probes **18a**−**18t**, which were purified by chromatography or recrystallization. The analogues **18u**−**18w** (Chart 2) were prepared from **11a** and *N*-ethyl-3-nitrobenzylamine, 1-(2-aminoethyl)-4-nitrobenzene, and (4-nitrophenyl)methanethiol (prepared by treatment of 4-nitrobenzyl bromide

Scheme 2. Synthesis of 4-(Substituted)benzylamines **14a**−**14j** and **17k**−**17t** and Inhibitors **18a**−**18t**[a]

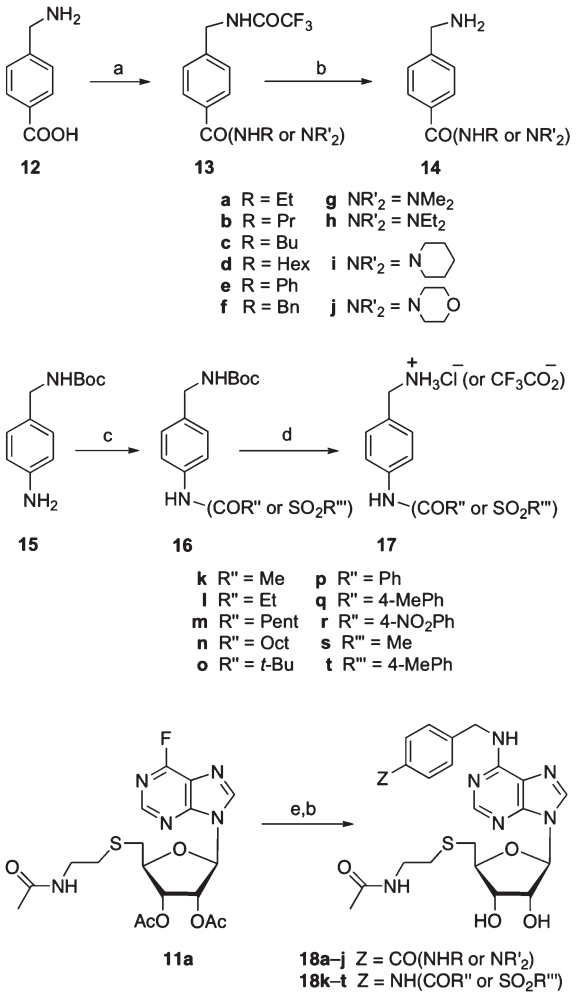

[a] Reagents and conditions: (a) (1) $(CF_3CO)_2O$, pyridine, CH_2Cl_2, 0 °C to ambient, (2) $SOCl_2$, CH_2Cl_2, ambient, (3) RNH_2 (or R'_2NH), CH_2Cl_2, 0 °C to ambient; (b) 30% NH_3/H_2O, MeOH, 60 C; (c) RCOCl, Et_3N, 0 °C (or RSO_2Cl, pyridine, ambient); (d) CF_3CO_2H, CH_2Cl_2 (or 37% HCl/H_2O, MeOH), ambient; (e) **14a**−**j** or **17k**−**t**), Et_3N, MeOH, ambient.

with potassium thioacetate followed by deacetylation), respectively.

NBAdo analogues with a free hydroxyl group at C5′ had shown large differences in the concentrations required for inhibition of nucleoside transporters of cultured mouse S49 lymphoma and L1210/B23.1 leukemia cells [Δ(nM) $>10^3$], and changes in the amide substituents at C4 of the phenyl ring of 6-*N*-benzyladenosine analogues also resulted in significant changes in the concentrations that inhibited binding of NBMPR with pig erythrocyte transporters by 50% [IC_{50} value Δ(μM) $>10^2$].[24] In marked contrast, transport of [^{3}H]uridine by recombinant hENT1 produced in yeast was observed at 57−87% of control values with 3 nM concentrations of **18a**−**18w** (Table 1 in the Supporting Information) and at 15−25% of control values at 10 nM. The 6-*S*-(4-nitrobenzyl) analogue **18w** was slightly more inhibitory than **18a**−**18v** at 3 nM, but the relative inhibitory difference was even smaller at 10 nM. It is noteworthy that almost no structural sensitivity for binding to hENT1-yeast was observed with the 5′-*S*-(2-acetamidoethyl)-5′-thio analogues **18a**−**18w** with 23 different 6-*N*-substituents. Because no

Chart 2. Structures of Inhibitors **18u**−**18w**

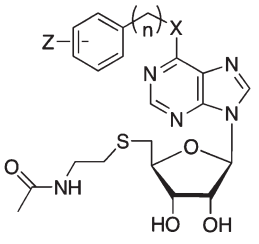

18u n = 1, X = NEt, Z = 3-NO_2
18v n = 2, X = NH, Z = 4-NO_2
18w n = 1, X = S, Z = 4-NO_2

Scheme 3. Synthesis of **3**, **28a**, Analogues, and FITC-Conjugates **5a**, **5b**, **7a**, and **7b**[a]

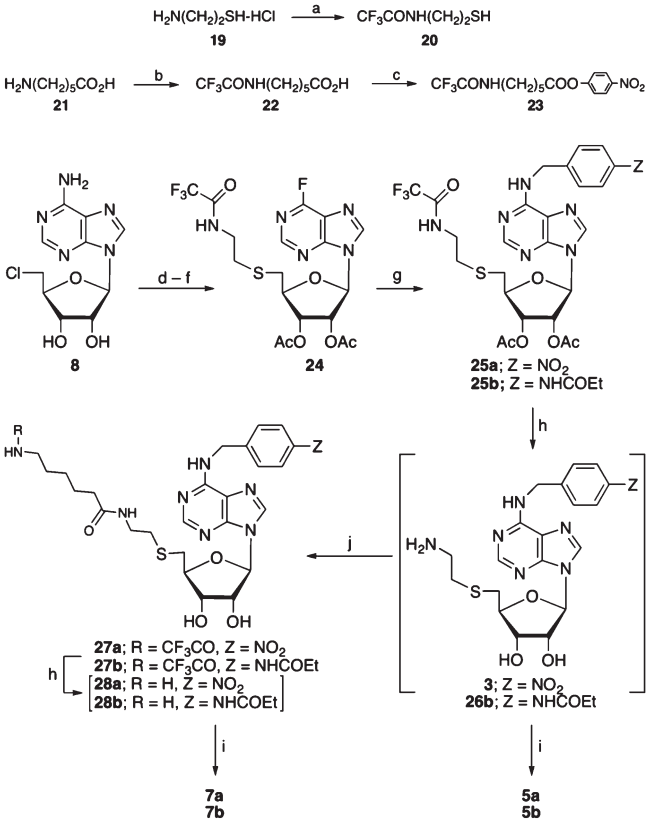

[a] Reagents and conditions: (a) $(CF_3CO)_2O$, pyridine, benzene, ambient; (b) $(CF_3CO)_2O$, 80 °C; (c) DCC, 4-nitrophenol, CH_2Cl_2, ambient; (d) **20**, NaH, DMF, ambient; (e) Ac_2O, pyridine, 0 °C; $NaNO_2$, ~55% HF-pyridine, −10 to −5 °C; (g) 4-nitrobenzylamine or **17l**, Et_3N, MeOH, ambient; (h) 30% NH_3/H_2O, MeOH, 60 °C; (i) FITC, Et_3N, DMF, ambient; (j) **23**, Et_3N, DMF, ambient.

SAR trend was observed, 4-nitrobenzyl and 4-(propanamido)-benzyl groups were selected for attachment at N6 of the fluorescent-conjugate targets. hENT1 exhibited enhanced affinity for the 4-nitrobenzyl moiety, and the 4-(propanamido)-benzyl analogue **18l** was bound well and does not contain a nitro group.

Trifluoroacetylation of 2-aminoethanethiol (**19**) (Scheme 3) gave 2-(trifluoroacetamido)ethanethiol (**20**). Treatment of **8** with the sodium thiolate derived from **20** gave the 5′-thioether, which was acetylated and subjected to fluoro-diazotization to give 9-{2,3-di-*O*-acetyl-5-*S*-[2-(trifluoroacetamido)ethyl]-5-thio-β-D-ribofuranosyl}-6-fluoropurine (**24**). The electron withdrawing trifluoroacetyl group on the amide nitrogen ameliorated the problematic formation of *N*-nitroso byproducts. S_NAr displacement of fluoride from **24** with 4-nitrobenzylamine and **17l** at ambient temperature gave **25a** and **25b**, respectively, which were deprotected (to give **3** and **26b**) and treated with FITC in Et_3N/DMF at ambient temperature to give **5a** (56%) and **5b** (95%), respectively.

Analogues with the extended spacer were then prepared. Enhanced fluorescent output was noted with **6**,[16] and probes with longer spacers between receptor-binding and fluorescent-reporting entities usually present fewer problems with fluorescence quenching. Trifluoroacetylation of 6-aminohexanoic acid (**21**) gave **22**, which was converted into its 4-nitrophenyl ester **23** with DCC and 4-nitrophenol. Treatment of **3** and **26b** with **23** in Et_3N/DMF gave the 5′-*S*-{2-[6-(trifluoroacetamido)hexanamido]ethyl}5′-thionucleoside derivatives **27a** and **27b**, respectively. Removal of the trifluoroacetyl group from **27a** and **27b** gave **28a** and **28b**. Treatment of crude **28a** and **28b** with FITC/Et_3N/DMF gave **7a** (86%) and **7b** (89%), respectively.

Nucleoside Transport

Development of a high-affinity fluorescent probe for rapid and efficient quantification of hENT1 sites on cell surfaces by flow cytometry that would be applicable for prediction of the transport of nucleoside analogue drugs into cancer (and viral-infected) cells was our primary goal. An additional goal was confocal-microscopy monitoring of the surface staining of hENT1 in living cells with native hENT1 and in various cellular expression systems that produce recombinant hENT1 proteins. Probes that identify cell-surface abundances of hENT1 would be useful in distinguishing between ENT1 proteins located in intracellular membranes from those that are located in plasma membranes and could potentially function in the transport of nucleosides into and/or out of cells.

Inhibition of [^{3}H]uridine transport was measured with yeast that were producing recombinant hENT1. NBMPR and **18a**−**18w** (each tested at 3 nM) reduced transport to 51−87% of control values (Table 1 in the Supporting Information). An arbitrary selection of 4-nitrobenzyl and 4-(propanamido)benzyl groups at N6 of our fluorescent probe targets was made because no SAR was observed for transport inhibition in this model system with the 23 analogues tested. Conjugation of **3** and **26b** with FITC gave the known **5a** and its 4-(propanamido)benzyl analogue **5b**. Conjugation of **28a** and **28b** with FITC gave the new extended-linker probes **7a** and **7b**, respectively.

The four fluorescein conjugates **5a**, **5b**, **7a**, and **7b** were assessed for their abilities to inhibit [^{3}H]uridine influx and [^{3}H]NBMPR binding in yeast producing recombinant hENT1. Uptake of [^{3}H]uridine (1 μM) was measured at ambient temperature during 20 min in the absence (control) or presence of a partially inhibitory concentration of unlabeled NBMPR (3 nM) or each of the four compounds **5a**, **5b**, **7a**, or **7b** (also at 3 nM). NBMPR reduced uridine transport by approximately 50%, whereas **5a**, **5b**, **7a**, and **7b** reduced uridine transport by 20−30%. Again, only small differences were observed among the four compounds (Figure 1A). Inhibition of binding of [^{3}H]NBMPR (5 nM) to recombinant hENT1 in yeast in the absence or presence of unlabeled NBMPR, **5a**, **5b**, **7a**, or **7b** (all at 500 nM) is shown in Figure 1B. It is noteworthy that the 4-nitrobenzyl compounds **5a** and **7a** exhibited much greater inhibition of binding of [^{3}H]NBMPR to hENT1 than their 4-(propanamido)benzyl analogues **5b** and **7b**.

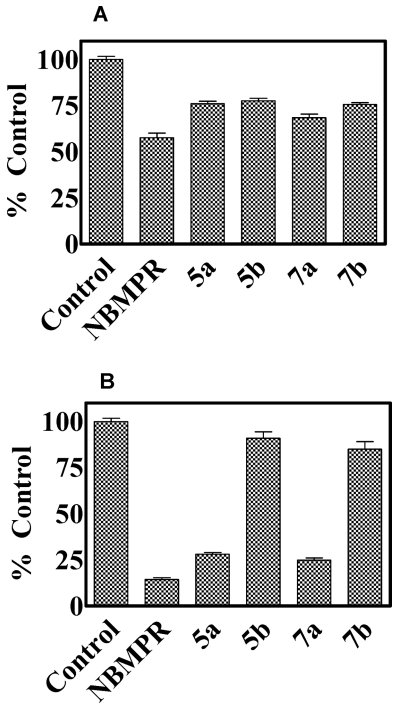

Figure 1. Inhibition of [^{3}H]uridine uptake and [^{3}H]NBMPR binding in yeast producing recombinant hENT1. (A) Uridine uptake. Uptake of [^{3}H]uridine (1 μM) was measured at ambient temperature during 20 min in the absence (control) or presence of unlabeled NBMPR (3 nM) or each of **5a**, **5b**, **7a**, or **7b** (3 nM). Uptake values in the presence of test compounds are expressed as percentages of values in their absence (control). Results from three independent experiments were used to calculate the SE values. (B) NBMPR binding. Binding of [^{3}H]NBMPR (5 nM) was measured in the absence or presence of 500 nM unlabeled NBMPR, **5a**, **5b**, **7a**, or **7b** for 60 min at ambient temperature and inhibition is plotted as percentages of values in the absence of text compounds (control). Results are the average of three independent experiments.

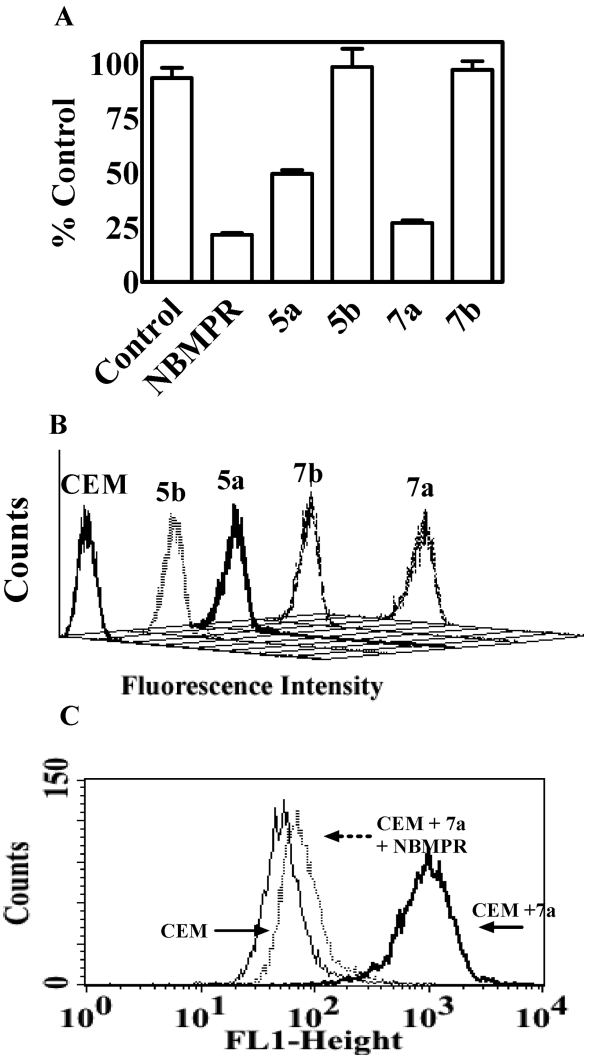

Figure 2. Interacttion of FITC conjugates with hENT1 on CEM cells. (A) Inhibition of binding of [^{3}H]NBMPR. Binding of [^{3}H]NBMPR (5 nM) was measured in the absence or presence of excess (500 nM) unlabeled NBMPR (or **5a**, **5b**, **7a**, or **7b**) as described in the Experimental Section (inhibition plotted as % control with no NBMPR, **5a**, **5b**, **7a**, or **7b**). Results are the average of two independent experiments. (B) Binding measured by flow cytometry. Shown are fluorescence histogram of the binding of **5a**, **5b**, **7a**, or **7b** with hENT1 on CEM cells treated with the respective analogue (100 nM) and incubated for 1 h. Cell-bound fluorescence was analyzed by flow cytometry as described. (C) Inhibition of binding of **7a** by NBMPR. CEM cells were treated with **7a** (0 or 100 nM) or [**7a** (100 nM) + NBMPR (1 μM)]. In the latter case, cells were preincubated with NBMPR for 10 min prior to the addition of **7a**. Results shown were from one representative experiment of three.

Inhibition of binding of [^{3}H]NBMPR (5 nM) to cultured human CEM lymphoblastoid leukemia cells in the presence of excess (500 nM) unlabeled NBMPR (or **5a**, **5b**, **7a**, or **7b**) was calculated as a percent of binding in the absence of an inhibitor and represented "total" specifically bound [^{3}H]NBMPR (control values). Figure 2A shows that FITC-SAHENTA (**7a**) produced the most potent inhibition, similar to that with unlabeled NBMPR. The four analogues were also subjected to experiments in which 2.5×10^5 CEM cells in phosphate-buffered saline (PBS) were incubated with the individual compounds (100 nM) for 1 h, and the cell-associated fluorescence was analyzed by flow cytometry. The highest fluorescence intensity was observed with **7a** (Figure 2B) in harmony with the results from inhibition of [^{3}H]NBMPR-binding with hENT1 in yeast (Figure 1B) and in CEM cells (Figure 2A). Binding of **7a** (100 nM) to CEM cells in the absence or presence of NBMPR (1 μM) was monitored by flow cytometry as described in the Experimental Section. Histograms of the cell-bound fluorescence (Figure 2C) show that the presence of NBMPR (1 μM) caused a reduction in the binding of **7a** to CEM cells similar to the fluorescence values observed with untreated cells. Similar to the results with recombinant hENT1 in yeast, the 4-nitrobenzyl compounds **5a** and **7a** exhibited two- to 4-fold greater inhibition of the binding of [^{3}H]NBMPR with CEM cells relative to their 4-(propanamido)benzyl analogues **5b** and **7b**, although only small differences had been observed (Figure 1A) in the inhibition of [^{3}H]uridine transport by recombinant hENT1 in yeast with **5a**, **5b**, **7a**, or **7b**.

Inhibition of the entry of [^{3}H]uridine (1 μM) into CEM cells by **7a** was assessed in 30 s time-course experiments and was found to be equivalent with the inhibition observed with 1-μM concentrations of either **7a** or unlabeled NBMPR (Figure 3A). Graded concentrations of **7a** (0−10 μM) produced dose-dependent inhibition of transport of [^{3}H]uridine (1 μM) in CEM cells with an effective concentration for 50% inhibition (EC_{50}) of 18 ± 4.7 nM (Figure 3B), which indicated high-affinity binding of **7a** by hENT1. Binding specificity for **7a** was assessed with graded concentration-dependent competitions by **7a** (0−1000 nM) against [^{3}H]NBMPR (10 nM) for

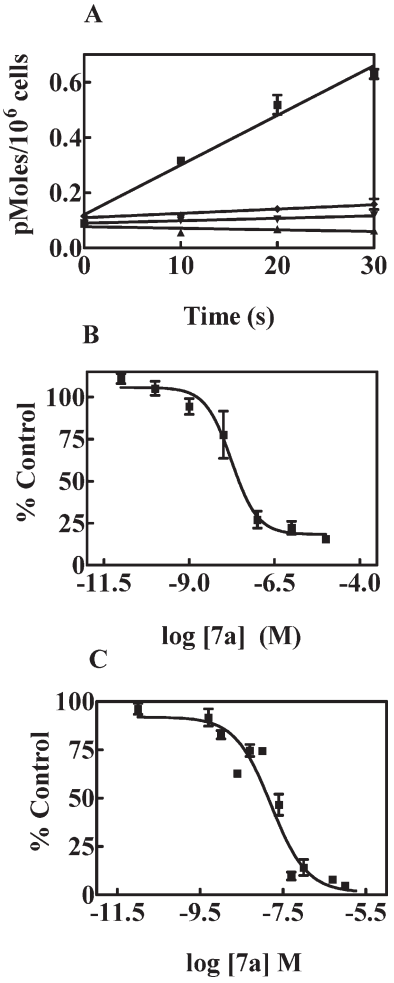

Figure 3. Inhibition of [^{3}H]uridine influx and [^{3}H]NBMPR binding by **7a**. (A) Uridine influx. Time courses of influx of [^{3}H]uridine (1 μM, ■) in CEM cells in the absence or presence of NBMPR (1 μM, ▲), **7a** (1 μM, ▼), or uridine (1 mM, ♦) was measured for 0−30 s. Plotted values were derived from two independent experiments. (B) Dose-dependent inhibition of uridine transport by **7a**. CEM cells were preincubated with graded concentrations of **7a** (0−10 μM) for 10 min, and [^{3}H]uridine transport was measured as described in the Experimental Section. Results derived from three independent experiments were plotted as % control (no **7a**). (C) Dose-dependent inhibition of NBMPR binding by **7a**. Inhibition of [^{3}H]NBMPR (10 nM) binding was measured after 1 h incubations of cells in the absence or presence of graded concentrations of **7a**. Specifically bound [^{3}H]NBMPR (expressed as % control that was bound in the absence of **7a**) was plotted as a function of **7a** concentrations (three experiments each performed with triplicates).

hENT1 sites on CEM cells. Figure 3C shows the inhibition of [^{3}H]NBMPR binding by **7a** with EC_{50} = 14 ± 4 nM.

CEM cells were incubated with different concentrations of **7a** (0−25 nM) in the absence or presence of NBMPR (1 μM) as described in the Experimental Section, and cell-associated fluorescence was analyzed by flow cytometry. Reaction volumes and cell numbers were maintained such that depletion of the concentrations of **7a** did not occur. Fluorescence intensities and the percentage of positive cells increased to saturation as a function of increasing concentrations of **7a**. NBMPR-sensitive binding values were obtained by subtraction of the fluorescence in the presence of excess NBMPR from that in the presence of **7a**, and the values (% gated × mean fluorescence intensities) were plotted against the initial concentrations of **7a** (Figure 4A). Half-maximal binding in these studies

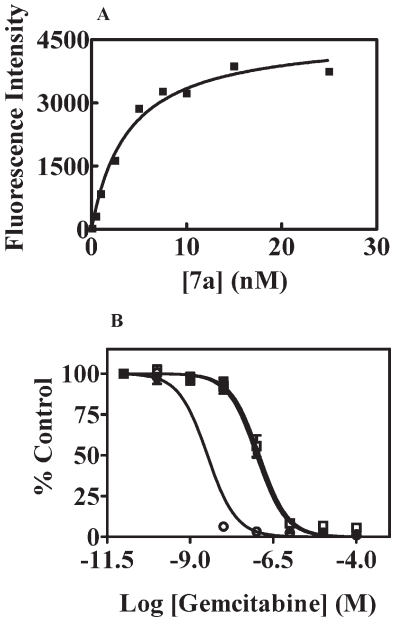

Figure 4. Equilibrium binding and protection from cytotoxicity with **7a**. (A) Equilibrium binding of **7a** with CEM cells. The mean channel fluorescence output at each of the concentrations of **7a** was multiplied by the number of positive cells, and the resulting values (expressed as fluorescence) were plotted as a function of the concentrations of **7a**. Values in the presence of NBMPR (1 μM) were subtracted from the total value, and the net fluorescence values were plotted for one representative experiment out of four. (B) Evaluation of **7a** as a protective agent against cytotoxicity. CEM cells were treated with gemcitabine (0−100 μM, ○) in the absence or presence of NBMPR (1 μM, ●) or **7a** (1 μM, □) for 72 h. Cells were pretreated with NBMPR or **7a** for 2 h prior to the addition of gemcitabine for the protection experiments. The results are averages of two independent experiments with six replicates each.

occurred when **7a** was at a concentration of ~4 ± 1 nM, a value that should approximate the K_d value for the specific binding of **7a** to the hENT1 sites on CEM cells because experiments were conducted under equilibrium-binding conditions (prolonged exposures, nondepleting conditions).

The abilities of NBMPR and **7a** to protect CEM cells against gemcitabine cytotoxicity were compared (Figure 4B) to determine if **7a** could function as an equivalent high-affinity inhibitor of hENT1-mediated transport of gemcitabine. Cells in 96-well plates were exposed to graded concentrations of gemcitabine (0−100 μM) in the absence or presence of NBMPR or **7a** (1 μM). Cells were incubated with NBMPR or **7a** for 1 h to allow saturation of binding to hENT1 before addition of graded concentrations of gemcitabine. NBMPR and **7a** each caused an approximately 30-fold protection against the cytotoxic effects of gemcitabine during extended drug exposures.

We evaluated the abundance of cell-surface hENT1 in six cancer cell lines of human or murine origin (S49, L1210, HL-60, CEM, K562, and BeWo) with known (and different) numbers of NBMPR binding sites by flow cytometry to assess whether **7a** was a viable candidate for prediction of hENT1 site densities before chemotherapy with nucleoside drugs. Cells were incubated with **7a** (100 nM) for 1 h at ambient temperature. The increases in fluorescence staining were roughly proportional to the known abundances of hENT1 with the cells tested (Figure 5A), which demonstrated that **7a** was a useful probe for quantification of hENT1 sites. Cell permeation is the initial barrier encountered by nucleoside

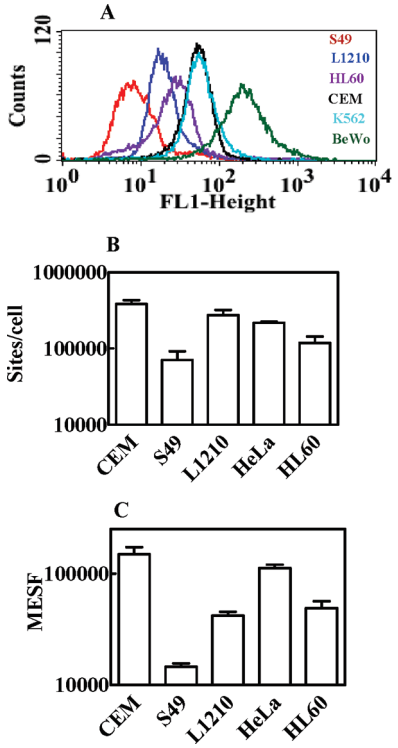

Figure 5. Evaluation of **7a** as a cell-surface probe. (A) Flow cytometry with cells with different numbers of hENT1 sites. S49, L1210, HL60, CEM, K562, and BeWo cells were incubated with **7a** (100 nM) for 1 h and the cell-bound fluorescence was measured by flow cytometry. (B) Quantification of hENT1 sites by site-specific binding of [^{3}H]NBMPR. The binding of [^{3}H]NBMPR with CEM, S49, L1210, HeLa, and HL60 cells was measured as described in the Experimental Section. The bar graph shows the numbers of sites/cell with the different cell lines. (C) Quantification of hENT1 sites using fluorescent beads. Flow cytometry with standardized fluorescent beads was used to quantitate the numbers of cell-surface hENT1 sites measured with **7a** for the CEM, S49, L1210, HeLa, and HL60 cell lines. The number of molecules of equivalent soluble fluorescein (MESF, as a measure of hENT1 sites) was plotted relative to each cell line (results are representative of four independent experiments).

analogues on their pathways to drug activity, and nucleoside transporters at cell surfaces mediate that first crucial process. We also evaluated whether **7a** was an impermeable surface probe because the smaller NBMPR molecule, which can enter cells by transport and/or diffusion,[17] reports both intracellular and cell surface hENT1 abundance.[29] Measurement of cell-associated [^{3}H]NBMPR gave a combined total of exobound hENT1 sites on plasma membranes plus hENT1 associated with intracellular membranes (Figure 5B), whereas flow cytometry with **7a** measured only the exobound sites (Figure 5C). The fluorescence densities observed with **7a** showed lower abundances of surface hENT1 sites on S49 and L1210 cells relative to the values obtained by counting cell-associated [^{3}H]NBMPR. The number of molecules of equivalent soluble fluorescein (MESF) bound to the cells was calibrated with fluorescent beads.

We also evaluated whether **7a** could be used to visualize hENT1 sites by fluorescence microscopy on three model cell systems used extensively for the characterization of hENT1. Cultured CEM cells with native hENT1 activity and yeast or *Xenopus* oocytes with recombinant hENT1 activity were individually incubated without or with **7a** (100 nM) in the absence or presence of NBMPR (1 μM) for 1 h and then

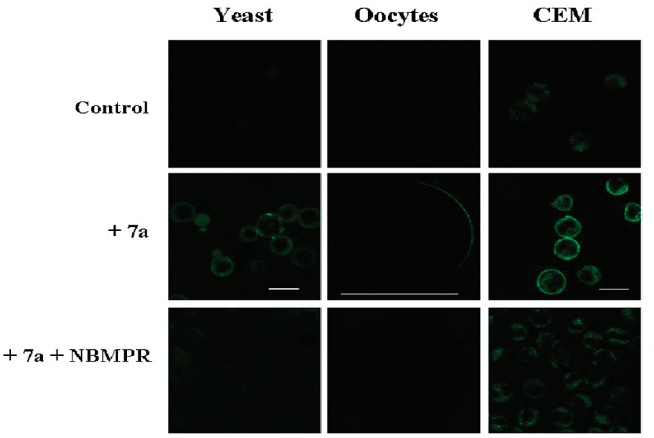

Figure 6. Confocal microscopic analysis of the staining of hENT1 sites with **7a**. CEM cells and recombinant hENT1-producing yeast and oocytes were incubated individually with **7a** (0 or 100 nM) in the absence or presence of NBMPR (1 μM) and spun down quickly. The pellets were resuspended in a small volume of phosphate-buffered saline, layered on coverslips coated with poly-L-lysine, and visualized immediately with a confocal microscope. Bright staining on the membranes indicates binding with **7a**.

processed as described in the Experimental Section. Parts A−C of Figure 6 show that specific cell-surface staining of hENT1 was observed.

Discussion and Summary

The protected 5′-*S*-(2-acetamidoethyl)-6-fluoropurine nucleoside **11a** underwent clean S_NAr displacement of fluoride with 4-(substituted)benzylamines, and the intermediates were deprotected to give the 5′-(2-acetamidoethyl)-6-*N*-[4-(substituted)benzyl)adenosine derivatives **18a**−**18w** that inhibited [^{3}H]uridine transport at nearly equivalent nanomolar levels with hENT1-containing yeast. S_NAr displacements with the 5′-*S*-(2-trifluoroacetamidoethyl)-6-fluoropurine nucleoside **24** and 4-nitrobenzylamine or 4-(propanamido)benzylamine followed by complete deprotection gave **3** or its propanamido analogue **26b**, respectively. Treatment of those crude 5′-*S*-(2-aminoethyl) intermediates with the 4-nitrophenyl (active) ester of 6-(trifluoroacetamido)hexanoic acid gave the 5′-*S*-{2-[6-(trifluoroacetamido)hexanamido]}ethyl-5′-thio compounds **27a** and **27b**. The four trifluoroacetamido intermediates were easily purified by flash chromatography, and aqueous methanolic ammonia at 60 °C effected removal of the trifluoroacetyl group to give amino compounds that did not require purification. Deprotection of **25a** and **25b** followed by treatment of the amino intermediates **3** and **26b** with FITC gave **5a** and **5b**, and treatment of **27a** and **27b** by the same two-stage sequence gave the extended-linker conjugates **7a** and **7b**. Conjugates **5a**, **5b**, **7a**, and **7b** were purified by flash chromatography, whereas HPLC was employed to remove persistent byproducts formed during prior syntheses that used alkylation/rearrangement and deprotection of a phthalimido intermediate.

The four fluorescein conjugates **5a**, **5b**, **7a**, and **7b** inhibited [^{3}H]uridine transport at nearly equivalent nanomolar levels, whereas they exhibited substantial differences in levels of inhibition of [^{3}H]NBMPR binding. Compounds **5a** and **7a** produced effects similar to those observed in the presence of excess nonradioactive NBMPR, whereas the effects of **5b** and **7b** were negligible. Similar results were observed in NBMPR-binding experiments with CEM cells in which **5a** and **7a**

produced 2−4-fold greater inhibition of NBMPR binding than **5b** and **7b**. Flow-cytometry experiments validated the efficacies of **5a** and **7a** as hENT1 probes. Conjugate **7a** showed the highest inhibition of NBMPR binding and yielded the highest fluorescence output when bound to CEM cells. Further characterization of **7a** was pursued with CEM cells, which are known to possess a single nucleoside transporter type (i.e., hENT1).[30] Flow cytometric experiments showed that binding of **7a** to hENT1 sites on CEM cells was inhibited by NBMPR, which indicated that the interaction of these two inhibitors with hENT1 sites was mutually exclusive. We also demonstrated that **7a** was a potent inhibitor of [^{3}H]uridine transport in CEM cells with an IC_{50} value of 17 nM for the inhibition of uridine influx. Binding of [^{3}H]NBMPR was inhibited by **7a** in a concentration-dependent manner with an IC_{50} value of 14 nM. Equilibrium binding was measured as a function of increasing concentrations of **7a** (0−25 nM), and a K_d value of 4 nM was calculated for binding of **7a** to hENT1 sites.

Passive diffusion and/or mediated transport of [^{3}H]NBMPR through cell membranes could result in measured counts that include association of [^{3}H]NBMPR with intracellular membranes, as has been shown previously,[15] as well as extracellular binding to hENT1. Erroneous predictions of drug response based on estimated hENT1 sites for facilitated nucleoside influx could result, and accumulation of [^{3}H]NBMPR might be amplified in tumors with increased cell permeabilities. We compared the relative levels of association of [^{3}H]NBMPR versus **7a** with S49 and L1210 cells. The larger [^{3}H]NBMPR values indicated that intracellular [^{3}H]NBMPR might also be present relative to the surface binding with **7a**. Recent studies with cultured pancreatic cell lines[31,32] showed a strong correlation between [^{3}H]3′-deoxy-3′-fluorothymidine (FLT) uptake and the number of extracellular NBMPR binding sites/cell, and the uptakes of FLT and gemcitabine were comparable in predicting gemcitabine toxicity in the pancreatic cancer cell lines tested.

NBMPR and **7a** provided similar protection of cells against the cytotoxic effects of gemcitabine, which indicated that they both interact at hENT1 sites (thereby inhibiting drug influx). Six different cell lines with different origins and numbers of hENT1 sites were analyzed by flow cytometry with **7a**, and higher levels of fluorescence were observed with cells that had greater hENT1 site densities. Definitive membrane staining was observed with **7a** and three model systems (yeast, oocytes, and cells) that produced hENT1, and this same approach was used to measure cell-surface hENT1 levels with CEM cells and yeast that produced mutant hENT1.[33,34] Staining of hENT1-producing cells with **7a** has also been correlated with transport of the positron emission tomography (PET) imaging agent FLT (used clinically to identify proliferating tumor cells) in the human cancer cell lines MCF-7, A549, U251, A498, and Capan-2.[31]

In summary, methodology has been developed for reliable syntheses of **3**, **28a**, analogues, and fluorescent-conjugate probes. The FITC conjugate **7a** at nanomolar levels has been validated as a cell-surface probe of hENT1 with several in vitro model systems using flow cytometry or confocal microscopy. It is a potentially useful tool for analysis of hENT1 mutations that affect protein targeting to the plasma membrane and regulation of hENT1 in response to different stimuli. Staining with **7a** enables rapid quantification of surface hENT1 sites, which makes this procedure applicable to clinical samples for initial prediction of expected responses to nucleoside drugs.

Experimental Section

Chemistry General. Reactions were run under an N_2 atmosphere unless stated otherwise. Glassware was flame-dried. Reagent-grade solvents were dried with a Glass Contour drying system equipped with cylinders of activated alumina. FT-NMR spectra were obtained with Varian 300 and 500 MHz spectrometers in the indicated solvents. Internal references for NMR spectra were: ^{1}H, $CDCl_3$ (7.27 ppm), MeOH-d_4 (4.87 ppm), and DMSO-d_6 (2.50 ppm). ^{13}C, $CDCl_3$ (77.23 ppm), MeOH-d_4 (49.15 ppm), and DMSO-d_6 (39.51 ppm). High-resolution mass spectra (HRMS) were obtained with a Joel SX 102A double focusing mass spectrometer with an HP-9000 workstation. UV spectra were obtained with an HP 845X UV−visible spectrophotometer. TLC was performed with Sobent Technologies Silica G/UV254 plates. Flash chromatography was performed with silica gel (32−63 μ) purchased from Bodman with the indicated reagent-grade solvents. Some of the compounds **18a**−**18w** were recrystallized after column chromatography; those that failed to crystallize were subjected to flash chromatography a second time before being tested as inhibitors of nucleoside transport. FITC (90% isomer I) was purchased from Aldrich. All of the nucleoside analogues tested as transport inhibitors were of >95% purity as determined by our reported TLC, UV, and high-field NMR methods.[35]

9-(2,3-Di-*O*-acetyl-5-chloro-5-deoxy-β-D-ribofuranosyl)-6-fluoropurine (9). Compound **8**[28] (200 mg, 0.7 mmol) was added to pyridine (2 mL) and Ac_2O (2 mL) at 0 °C. The solution was stirred for 4 h at 0 °C and volatiles were evaporated. Flash chromatography of the residue (2 → 5% MeOH/CH_2Cl_2) gave 2′,3′-di-*O*-acetyl-5′-chloro-5′-deoxyadenosine (160 mg, 62%) as a white solid: UV (MeOH) max 261 nm, min 235 nm. ^{1}H NMR (DMSO-d_6, 500 MHz) δ 8.39 (s, 1H), 8.19 (s, 1H), 7.39 (br s, 2H), 6.25 (d, J = 6.0 Hz, 1H), 6.09 (t, J = 5.8 Hz, 1H), 5.63 (dd, J = 4.0, 5.5 Hz, 1H), 4.38−4.41 (m, 1H), 4.05 (dd, J = 5.3, 12.3 Hz, 1H), 3.97 (dd, J = 6.5, 12.0 Hz, 1H), 2.13 (s, 3H), 2.02 (s, 3H). ^{13}C NMR (DMSO-d_6, 125 MHz) δ 169.4, 169.2, 156.2, 152.9, 149.1, 139.9, 119.1, 85.2, 81.3, 71.7, 70.9, 43.8, 20.4, 20.1. HRMS (FAB) m/z 369.0840 (M^+ [$C_{14}H_{16}ClN_5O_5$] = 369.0840).

$NaNO_2$ (180 mg, 2.61 mmol) was added to a stirred solution of the diacetate (200 mg, 0.54 mmol) in ∼55% HF-pyridine (1.8 mL) at −25 °C. Stirring was continued while the temperature was allowed to rise slowly to 0 °C. Ice−water was added, the mixture was extracted (CH_2Cl_2), the combined organic phase was washed (5% $NaHCO_3$/H_2O and then H_2O), and volatiles were evaporated under vacuum. Flash chromatography of the residue (80% EtOAc/hexanes) gave **9** (173 mg, 86%) as a white solid foam: UV (MeOH) max 239 nm, min 217 nm. ^{1}H NMR ($CDCl_3$, 500 MHz) δ 8.66 (s, 1H), 8.36 (s, 1H), 6.30 (d, J = 6.0 Hz, 1H), 5.93 (t, J = 6.0 Hz, 1H), 5.66 (dd, J = 3.8, 5.8 Hz, 1H), 4.52 (dd, J = 4.0, 8.0 Hz, 1H), 3.93 (dd, J = 4.3, 11.8 Hz, 1H), 3.89 (dd, J = 4.5, 12.0 Hz, 1H), 2.17 (s, 3H), 2.06 (s, 3H). ^{13}C NMR (DMSO-d_6, 125 MHz) δ 169.3, 169.2, 158.9 (d, J = 256.3 Hz), 155.0 (d, J = 10.7 Hz), 151.9 (d, J = 14.5 Hz), 146.0, 120.0 (d, J = 29.7 Hz), 86.0, 81.5, 72.0, 70.6, 43.7, 20.3, 20.1. HRMS (FAB) m/z 373.0708 (MH^+ [$C_{14}H_{15}ClFN_4O_5$] = 373.0715).

5′-*S*-(2-Acetamidoethyl)-5′-thioadenosine (10). NaH (60% in mineral oil, 1.34 g, 33.5 mmol) was added to a solution of 2-acetamidoethanethiol (3.40 g, 28.6 mmol) in DMF (120 mL) at 0 °C. Stirring was continued for ∼10 min at 0 °C until bubble evolution ceased, and **8**[28] (5.00 g, 17.5 mmol) was added. The mixture was stirred at 70 °C until the conversion to **10** was complete (TLC) and volatiles were evaporated under vacuum. Flash chromatography of the residue (10 → 20% MeOH/CH_2Cl_2) gave **10** (5.96 g, 92%) as a white solid: UV (MeOH) max 260 nm, min 229 nm. ^{1}H NMR (DMSO-d_6, 500 MHz) δ 8.34 (s, 1H), 8.15 (s, 1H), 7.92 (t, J = 5.0 Hz, 1H), 7.27 (s, 2H),

5.89 (d, J = 6.0 Hz, 1H), 5.48 (d, J = 6.0 Hz, 1H), 5.30 (d, J = 5.0 Hz, 1H), 4.74 (dd, J = 6.0, 11.0 Hz, 1H), 4.14 (dd, J = 4.8, 8.8 Hz, 1H), 3.98−4.02 (m, 1H), 3.17 (dd, J = 7.0, 13.0 Hz, 2H), 2.92 (dd, J = 5.8, 14.3 Hz, 1H), 2.84 (dd, J = 7.3, 13.8 Hz, 1H), 2.56 (dt, J = 2.0, 6.8 Hz, 2H), 1.78 (s, 3H). ^{13}C NMR (DMSO-d_6, 125 MHz) δ 169.1, 156.1, 152.6, 149.4, 139.8, 119.1, 87.3, 83.8, 72.6, 72.5, 38.6, 33.9, 31.4, 22.5. HRMS (FAB) m/z 391.1183 (MNa^+ [$C_{14}H_{20}N_6O_4SNa$] = 391.1164).

9-[5-*S*-(2-Acetamidoethyl)-2,3-di-*O*-acetyl-5-thio-β-D-ribofuranosyl]-6-fluoropurine (11a) and 9-{2,3-Di-*O*-acetyl-5-*S*-[2-(*N*-nitrosoacetamido)ethyl]-5-thio-β-D-ribofuranosyl}-6-fluoropurine (11b). A mixture of **10** (10.0 g, 27.1 mmol) in pyridine (100 mL) and Ac_2O (24 mL) at 0 °C was stirred for 2 h at 0 °C. Ice and MeOH were added and volatiles were removed under vacuum. Flash chromatography of the residue (5 → 20% MeOH/CH_2Cl_2) gave 2′,3′-di-*O*-acetyl-5′-*S*-(2-acetamidoethyl)-5′-thioadenosine (11 g, 90%) as a white solid foam: UV (MeOH) max 258 nm, min 227 nm. ^{1}H NMR (DMSO-d_6, 500 MHz) δ 8.40 (s, 1H), 8.19 (s, 1H), 7.92 (t, J = 5.5 Hz, 1H), 7.38 (s, 2H), 6.19 (d, J = 6.0 Hz), 6.10 (t, J = 5.8 Hz, 1H), 5.56 (dd, J = 4.3, 5.8 Hz, 1H), 4.26−4.30 (m, 1H), 3.17 (dd, J = 6.8, 12.8 Hz, 2H), 3.04 (dd, J = 5.8, 14.3 Hz, 1H), 2.99 (dd, J = 7.3, 13.8 Hz, 1H), 2.57 (dt, J = 2.5, 6.8 Hz, 2H), 2.13 (s, 3H), 2.01 (s, 3H), 1.78 (s, 3H). ^{13}C NMR (DMSO-d_6, 125 MHz) δ 169.5, 169.3, 169.2, 156.2, 152.9, 149.1, 140.0, 119.2, 85.2, 81.5, 72.2, 71.8, 38.5, 33.1, 31.4, 22.5, 20.4, 20.2. HRMS (EI) m/z 452.1495 (M^+ [$C_{18}H_{24}N_6O_6S$] = 452.1478).

$NaNO_2$ (160 mg, 2.32 mmol) was added to a solution of the diacetate (700 mg, 1.55 mmol) in ∼55% HF-pyridine (6 mL) at −10 °C and the mixture was stirred for 1.5 h at −10 to −5 °C. Ice−water was added and the mixture was extracted (CH_2Cl_2). The combined organic phase was washed (5% $NaHCO_3/H_2O$ and then H_2O) and volatiles were removed under vacuum. Flash chromatography of the residue (EtOAc → 5% MeOH/EtOAc) gave **11a** (450 mg, 64%) as a white solid foam and **11b** (180 mg, 24%) as light-yellow oil. **11a**: UV (MeOH) max 237 nm, min 221 nm. ^{1}H NMR ($CDCl_3$, 500 MHz) δ 8.62 (s, 1H), 8.36 (s, 1H), 6.29 (t, J = 5.3 Hz, 1H), 6.20 (d, J = 4.5 Hz, 1H), 5.94 (t, J = 5.5 Hz, 1H), 5.59 (t, J = 5.3 Hz, 1H), 4.39 (dd, J = 4.8, 10.8 Hz, 1H), 3.31−3.42 (m, 2H), 3.04 (dd, J = 4.8, 14.8 Hz, 1H), 2.95 (dd, J = 6.0, 14.0 Hz, 1H), 2.62−2.71 (m, 2H), 2.12 (s, 3H), 2.03 (s, 3H), 1.93 (s, 3H). ^{13}C NMR ($CDCl_3$, 125 MHz) δ 170.5, 169.8, 169.5, 160.0 (d, J = 261.0 Hz), 155.0 (d, J = 11.4 Hz), 152.3 (d, J = 14.6 Hz), 144.1, 121.1 (d, J = 28.9 Hz), 86.8, 82.4, 73.1, 72.3, 38.7, 33.9, 32.9, 23.2, 20.7, 20.4. HRMS (FAB) m/z 478.1165 (MNa^+ [$C_{18}H_{22}FN_5O_6SNa$] = 478.1173). **11b**: UV (MeOH) max 238 nm, min 215 nm. ^{1}H NMR ($CDCl_3$, 500 MHz) δ 8.64 (s, 1H), 8.30 (s, 1H), 6.18 (d, J = 5.0 Hz, 1H), 5.92 (t, J = 5.3 Hz, 1H), 5.59 (t, J = 5.8 Hz, 1H), 4.38 (dd, J = 5.0, 11.0 Hz, 1H), 3.82−3.91 (m, 2H), 3.01 (dd, J = 5.0, 14.0 Hz, 1H), 2.97 (dd, J = 6.3, 14.0 Hz, 1H), 2.70 (s, 3H), 2.41−2.53 (m, 2H), 2.12 (s, 3H), 2.04 (s, 3H). ^{13}C NMR ($CDCl_3$, 125 MHz) δ 174.4, 169.7, 169.5, 160.0 (d, J = 261.0 Hz), 155.0 (d, J = 11.4 Hz), 152.3 (d, J = 13.7 Hz), 144.0, 121.2 (d, J = 28.9 Hz), 87.1, 82.6, 73.2, 72.3, 37.4, 33.8, 29.0, 22.5, 20.6, 20.4. HRMS (FAB) m/z 485.1255 (MH^+ [$C_{18}H_{22}FN_6O_7S$] = 485.1255).

Procedure A: General Method for Synthesis of 13a−13j. Example: *N*-Butyl-4-[(trifluoroacetamido)methyl]benzamide (13c). 4-(Aminomethyl)benzoic acid (**12**; 1.00 g, 6.61 mmol) was added to a stirred solution of dried CH_2Cl_2 (15 mL) and pyridine (2.14 mL, 2.10 g, 2.66 mmol) at 0 °C. Trifluoroacetic anhydride (1.87 mL, 2.78 g, 13.2 mmol) was slowly added and stirring was continued for 2 h at ambient temperature. Volatiles were removed under vacuum, $SOCl_2$ (5 mL) was added, and the mixture was stirred for 3 h at ambient temperature. Excess $SOCl_2$ was removed under vacuum and the residue was dissolved (CH_2Cl_2). The solution was cooled in an ice-bath and butylamine was slowly added until no further heat was produced (excess butylamine was added to ensure complete amide formation). The mixture was stirred overnight at ambient temperature and volatiles were removed under vacuum. Flash chromatography of the residue (30 → 50% EtOAc/hexanes) gave **13c** (1.62 g, 81%) as a white solid. ^{1}H NMR ($CDCl_3$, 500 MHz) δ 7.67 (d, J = 8.0 Hz, 2H), 7.27 (d, J = 7.5 Hz, 2H), 7.18 (br s, 1H), 6.17 (br s, 1H), 4.56 (d, J = 5.5 Hz, 2H), 3.43−3.47 (m, 2H), 1.57−1.63 (m, 2H), 1.41 (hex, J = 7.5 Hz, 2H), 0.96 (t, J = 7.5 Hz, 3H). HRMS (FAB) m/z 325.1126 (MNa^+ [$C_{14}H_{17}F_3N_2O_2Na$] = 325.1140).

Procedure B: General Method for Deprotection of 13a−13j. Example: 4-(Aminomethyl)-*N*-butylbenzamide (14c). Compound **13c** (800 mg, 2.65 mmol) was mixed with MeOH (5 mL) and 30% NH_3/H_2O (5 mL) in a sealed pressure tube and the mixture was heated at 60 °C until deprotection was complete (∼8 h, TLC). Volatiles were removed under vacuum to give **14c**. HRMS (EI) m/z 206.1414 (M^+ [$C_{12}H_{18}N_2O$] = 206.1419). The crude product mixture was used directly in the next step for S_NAr displacement with **11a.**

Procedure C: General Method for Synthesis of 16k−16t. Example: *tert*-Butyl *N*-[4-(Acetamido)benzyl]carbamate (16k). *tert*-Butyl *N*-(4-aminobenzyl)carbamate (**15**) (1.00 g, 4.50 mmol) was mixed with Et_3N (3.10 mL, 2.25 g, 22.3 mmol) and CH_2Cl_2 (15 mL), and the solution was cooled in an ice-bath. Acetyl chloride (480 μL, 530 mg, 6.75 mmol) was slowly added over ∼2 min, and the mixture was stirred at 0 °C until acetylation was complete (∼10 min, TLC). The mixture was then washed (H_2O) and volatiles were evaporated under vacuum. Flash chromatography of the residue (50% EtOAc/hexanes) gave **16k** (1.13 g, 95%) as a white solid. ^{1}H NMR ($CDCl_3$, 500 MHz) δ 7.46 (d, J = 8.0 Hz, 2H), 7.24 (d, J = 8.0 Hz, 2H), 7.17 (br s, 1H), 4.81 (br s, 1H), 4.27 (s, 2H), 2.19 (s, 3H), 1.46 (s, 9H). HRMS (FAB) m/z 287.1374 (MNa^+ [$C_{14}H_{20}N_2O_3Na$] = 287.1372).

Procedure D: General Method for Removal of the *t*-BOC Protecting Group from 16k−16t. Example: 4-(Acetamido)benzylamine (17k) Hydrotrifluoroacetate. Compound **16k** (350 mg, 1.33 mmol) was dissolved in CH_2Cl_2 (5 mL), and the stirred solution was cooled to 0 °C. Trifluoroacetic acid (TFA, 2 mL) was added and stirring was continued for 2 h at ambient temperature. Volatiles were removed under vacuum and the resulting yellow oil solidified upon addition of dried Et_2O. Filtration gave the light-yellow TFA salt of **17k**. Neutralization (Et_3N) of a sample of this material gave TLC-clean **17k**. HRMS (EI) m/z 164.0950 (M^+ [$C_9H_{12}N_2O$] = 164.0950).

Procedure E: Alternative Removal of the *t*-BOC Group. Example: 4-(Nonanamido)benzylamine (17n). HCl/H_2O (37%, 3 mL) was added to a stirred solution of **16n** (900 mg, 2.49 mmol) in MeOH (5 mL), and stirring was continued for 18 h at ambient temperature. Volatiles were removed under vacuum, Et_3N was added, and volatiles were removed under vacuum. The residue was dissolved (CH_2Cl_2), the solution was washed (1 M KOH/H_2O), and volatiles were evaporated under vacuum. Recrystallization of the residue (Et_2O/hexanes) gave white solid **17n** that was used directly for S_NAr displacement with **11a**.

Procedure F: General Method for Synthesis of 18a−18w. Example: 5′-*S*-(2-Acetamidoethyl)-6-*N*-[4-(*N*-propylcarbamoyl)-benzyl]-5′-thioadenosine (18b). Crude 4-(aminomethyl)-*N*-propylbenzamide **14b** {HRMS (EI) m/z 192.1267, M^+ [$C_{11}H_{16}N_2O$] = 192.1263; from procedure B with **13b** (∼1.87 mmol)} was mixed with **11a** (430 mg, 0.95 mmol) in MeOH (5 mL). Et_3N (262 μL, 190 mg, 1.88 mmol) was added, the solution was stirred for 4 h at ambient temperature, and volatiles were removed under vacuum. Flash chromatography of the residue (5 → 10% MeOH/CH_2Cl_2) gave a product that was mixed with MeOH (5 mL) and 30% NH_3/H_2O (5 mL) in a sealed pressure tube. The mixture was stirred for 1 h at 60 °C, and volatiles were evaporated under vacuum. Flash chromatography of the residue (5 → 10% MeOH/CH_2Cl_2) gave a product (440 mg, 86%) that was recrystallized (MeOH) to give white solid **18b**. UV (MeOH) max 267 nm (ε 23 500), min 241 nm (ε 13 800). ^{1}H NMR (DMSO-d_6, 500 MHz) δ 8.48 (br s, 1H), 8.40 (s, 1H), 8.36

(t, J = 5.5 Hz, 1H), 8.21 (s, 1H), 7.94 (t, J = 5.5 Hz, 1H), 7.75 (d, J = 8.5 Hz, 2H), 7.39 (d, J = 8.0 Hz, 2H), 5.90 (d, J = 6.0 Hz, 1H), 5.51 (d, J = 4.5 Hz, 1H), 5.34 (br s, 1H), 4.75 (br s, 3H), 4.14 (br s, 1H), 4.00 (dt, J = 4.0, 6.5 Hz, 1H), 3.15−3.21 (m, 4H), 2.92 (dd, J = 5.8, 13.8 Hz, 1H), 2.84 (dd, J = 7.3, 13.8 Hz, 1H), 2.56 (dt, J = 2.5, 7.0 Hz, 2H), 1.78 (s, 3H), 1.50 (hex, J = 7.0 Hz, 2H), 0.87 (t, J = 7.5 Hz, 3H). ^{13}C NMR (DMSO-d_6, 125 MHz) δ 169.1, 166.0, 154.4, 152.5, 148.9, 143.1, 140.0, 133.2, 127.1, 126.7, 119.6, 87.4, 83.8, 72.6, 72.5, 42.7, 40.9, 38.6, 33.9, 31.4, 22.5, 22.4, 11.4. HRMS (FAB) m/z 566.2149 (MNa^+ [$C_{25}H_{33}N_7O_5SNa$] = 566.2162).

(2-Trifluoroacetamido)ethanethiol (20). Thoroughly powdered 2-aminoethanethiol hydrochloride (**19**) (3.0 g, 26 mmol) was mixed with pyridine (5.2 mL) in dried benzene (40 mL). Trifluoroacetic anhydride (4.40 mL, 6.54 g, 31.2 mmol) was slowly added to the stirred mixture, and stirring was continued overnight at ambient temperature. Careful addition of 0.5 M Na_2CO_3/H_2O was followed by extraction ($CHCl_3$) of the aqueous layer and removal of volatiles from the combined organic layers under vacuum. Flash chromatography of the residue (30% EtOAc/hexanes) gave **20** (4.0 g, 88%). ^{1}H NMR (DMSO-d_6, 500 MHz) δ 9.52 (br s, 1H), 3.35 (q, J = 6.5 Hz, 2H), 2.59−2.64 (m, 2H), 2.50 (t, J = 8.0 Hz, 1H). HRMS (EI) m/z 172.0032 ($M^+ - H$ [$C_4H_5F_3NOS$] = 172.0044).

9-{2,3-Di-*O*-acetyl-5-*S*-[2-(trifluoroacetamido)ethyl]-5-thio-β-D-ribofuranoyl}-6-fluoropurine (24). NaH (60% in mineral oil, 0.18 g, 4.5 mmol) was added to a stirred solution of **20** (730 mg, 4.2 mmol) in DMF (20 mL) at 0 °C and stirring was continued for ~5 min at 0 °C (until evolution of gas bubbles ceased). 5′-Chloro-5′-deoxyadenosine[28] (**8**) (1.0 g, 3.5 mmol) was added, the mixture was stirred for 20 h at ambient temperature, and volatiles were evaporated under vacuum. Flash chromatography of the residue (10 → 20% MeOH/CH_2Cl_2) gave 5′-*S*-[2-(trifluoroacetamido)ethyl]-5′-thioadenosine (1.29 g, 87%): UV (MeOH) max 258 nm, min 229 nm. ^{1}H NMR (DMSO-d_6, 500 MHz) δ 9.48 (br s, 1H), 8.34 (s, 1H), 8.15 (s, 1H), 7.27 (s, 2H), 5.89 (d, J = 6.0 Hz, 1H), 5.49 (d, J = 6.5 Hz, 1H), 5.31 (d, J = 5.5 Hz, 1H), 4.74 ("q", J = 5.5 Hz, 1H), 4.14 (dd, J = 5.3, 9.3 Hz, 1H), 4.01 (dt, J = 4.0, 6.5 Hz, 1H), 3.32−3.37 (m, 2H), 2.94 (dd, J = 6.0, 13.5 Hz, 1H), 2.86 (dd, J = 7.3, 13.8 Hz, 1H), 2.63−2.72 (m, 2H). ^{13}C NMR (DMSO-d_6, 125 MHz) δ 156.3 (q, J = 36.3 Hz), 156.1, 152.7, 149.5, 139.9, 119.2, 115.9 (q, J = 288.1 Hz), 87.4, 83.8, 72.62, 72.60, 38.9, 33.7, 30.3. HRMS (FAB) m/z 445.0884 (MNa^+ [$C_{14}H_{17}F_3N_6O_4SNa$] = 445.0882).

That material (200 mg, 0.47 mmol) was added to a stirred solution of pyridine (3 mL) and Ac_2O (1 mL) at 0 °C and stirring was continued for 1.5 h at 0 °C. Ice and MeOH were added and then volatiles were removed under vacuum. Flash chromatography of the residue (3 → 5% MeOH/CH_2Cl_2) gave 2′,3′-di-*O*-acetyl-5′-*S*-[2-(trifluoroacetamido)ethyl]-5′-thioadenosine (210 mg, 87%): UV (MeOH) max 258 nm, min 227 nm. ^{1}H NMR (DMSO-d_6, 500 MHz) δ 9.47 (t, J = 5.5 Hz, 1H), 8.39 (s, 1H), 8.18 (s, 1H), 7.37 (s, 2H), 6.19 (d, J = 6.5 Hz, 1H), 6.10 (t, J = 6.0 Hz, 1H), 5.56 (dd, J = 4.3, 5.8 Hz, 1H), 4.27−4.31 (m, 1H), 3.32−3.36 (m, 2H), 3.05 (dd, J = 5.5, 14.0 Hz, 1H), 3.00 (dd, J = 7.0, 14.0 Hz, 1H), 2.68 (dt, J = 2.5, 7.0 Hz, 2H), 2.12 (s, 3H), 2.01 (s, 3H). ^{13}C NMR (DMSO-d_6, 125 MHz) δ 169.4, 169.2, 156.3 (q, J = 35.8 Hz), 156.2, 152.9, 149.1, 140.0, 119.2, 115.9 (q, J = 288.1 Hz), 85.3, 81.5, 72.2, 71.8, 38.8, 33.0, 30.3, 20.4, 20.2. HRMS (FAB) m/z 529.1090 (MNa^+ [$C_{18}H_{21}F_3N_6O_6SNa$] = 529.1093).

That material (1.25 g, 2.45 mmol) was dissolved in ~55% HF-pyridine (12 mL) at −10 °C, $NaNO_2$ (423 mg, 6.13 mmol) was added, and the mixture was stirred for 2 h at −10 to −5 °C. Ice−water was added, and the mixture was extracted (CH_2Cl_2). The combined organic phase was washed (5% $NaHCO_3/H_2O$ and then H_2O), and volatiles were removed under vacuum. Flash chromatography of the residue (80% EtOAc/hexanes → EtOAc) gave **24** (810 mg, 65%): UV (MeOH) max 240 nm, min 221 nm. ^{1}H NMR (DMSO-d_6, 500 MHz) δ 9.46 (t, J = 5.5 Hz, 1H), 8.92 (s, 1H), 8.76 (s, 1H), 6.37 (d, J = 5.5 Hz, 1H), 6.08 (t, J = 5.3 Hz, 1H), 5.60−5.62 (m, 1H), 4.36 (dd, J = 5.5, 11.5 Hz, 1H), 3.32 (dd, J = 7.0, 12.5 Hz, 2H), 3.07 (dd, J = 5.8, 14.3 Hz, 1H), 3.03 (dd, J = 7.0, 14.0 Hz, 1H), 2.67 (dt, J = 3.0, 7.0 Hz, 2H), 2.13 (s, 3H), 2.02 (s, 3H). ^{13}C NMR (DMSO-d_6, 125 MHz) δ 169.4, 169.3, 159.0 (d, J = 256.4 Hz), 156.3 (q, J = 36.1 Hz), 155.0 (d, J = 11.4 Hz), 151.9 (d, J = 33.0 Hz), 146.2, 120.2 (d, J = 29.8 Hz), 115.9 (q, J = 288.1), 86.1, 81.9, 72.08, 72.06, 38.8, 32.8, 30.3, 20.4, 20.2. HRMS (FAB) m/z 510.1062 (MH^+ [$C_{18}H_{20}F_4N_5O_6S$] = 510.1070).

2′,3′-Di-*O*-acetyl-6-*N*-(4-nitrobenzyl)-5′-*S*-[(2-trifluoroacetamido)ethyl]-5′-thioadenosine (25a). Et_3N (0.36 mL, 260 mg, 2.6 mmol) was added to a stirred mixture of **24** (380 mg, 0.75 mmol) and 4-nitrobenzylamine hydrochloride (210 mg, 1.1 mmol) in MeOH (3 mL), stirring was continued for 1 h at ambient temperature, and volatiles were removed under vacuum. Flash chromatography of the residue (50% EtOAc/hexanes → EtOAc) gave **25a** (420 mg, 88%): UV (MeOH) max 265 nm, min 227 nm. ^{1}H NMR (DMSO-d_6, 500 MHz) δ 9.48 (t, J = 5.3 Hz, 1H), 8.69 (br s, 1H), 8.46 (s, 1H), 8.25 (s, 1H), 8.17 (d, J = 9.0 Hz, 2H), 7.59 (d, J = 9.0 Hz, 2H), 6.22 (d, J = 6.0 Hz, 1H), 6.11 (t, J = 5.8 Hz, 1H), 5.57 (t, J = 5.0 Hz, 1H), 4.81 (d, J = 4.5 Hz, 2H), 4.28−4.31 (m, 1H), 3.33 (dd, J = 7.0, 13.0 Hz, 2H), 3.05 (dd, J = 5.8, 14.3 Hz, 1H), 3.00 (dd, J = 7.0, 14.0 Hz, 1H), 2.67 (dd, J = 1.5, 6.8 Hz, 2H), 2.12 (s, 3H), 2.02 (s, 3H). ^{13}C NMR (DMSO-d_6, 125 MHz) δ 169.5, 169.3, 156.3 (q, J = 35.6 Hz), 154.3, 152.8, 148.6, 148.1, 146.4, 140.5, 128.1, 123.5, 119.8, 115.9 (q, J = 286.5 Hz), 85.4, 81.5, 72.2, 71.8, 42.7, 38.9, 33.0, 30.3, 20.4, 20.2. HRMS (FAB) m/z 664.1417 (MNa^+ [$C_{25}H_{26}F_3N_7O_8SNa$] = 664.1413).

2′,3′-Di-*O*-acetyl-6-*N*-[4-(propanamido)benzyl]-5′-*S*-[(2-trifluoroacetamido)ethyl]-5′-thioadenosine (25b). Et_3N (0.55 mL, 400 mg, 3.96 mmol) was added to a stirred mixture of **24** (870 mg, 1.71 mmol) and the TFA salt of **17l** (600 mg, 2.05 mmol) in MeOH (5 mL), stirring was continued for 3 h at ambient temperature, and volatiles were removed under vacuum. Flash chromatography of the residue (80% EtOAc/hexanes → EtOAc → 10% MeOH/EtOAc) gave **25b** (840 mg, 73%): UV (MeOH) max 266 nm, min 241 nm. ^{1}H NMR (DMSO-d_6, 500 MHz) δ 9.78 (s, 1H), 9.46 (t, J = 5.5 Hz, 1H), 8.42 (br s, 1H), 8.41 (s, 1H), 8.24 (s, 1H), 7.49 (d, J = 8.5 Hz, 2H), 7.25 (d, J = 8.5 Hz, 2H), 6.20 (d, J = 6.5 Hz, 1H), 6.10 (t, J = 5.8 Hz, 1H), 5.56 (dd, J = 4.3, 6.8 Hz, 1H), 4.64 (br s, 2H), 4.27−4.30 (m, 1H), 3.34 (dd, J = 6.8, 14.3 Hz, 2H), 3.05 (dd, J = 5.8, 14.3 Hz, 1H), 3.00 (dd, J = 7.0, 14.0 Hz, 1H), 2.68 (dt, J = 2.0, 7.0 Hz, 2H), 2.28 (q, J = 7.5 Hz, 2H), 2.12 (s, 3H), 2.01 (s, 3H), 1.05 (t, J = 7.5 Hz, 3H). ^{13}C NMR (DMSO-d_6, 125 MHz) δ 171.7, 169.4, 169.2, 156.2 (q, J = 35.8 Hz), 154.4, 152.8, 148.4, 140.0, 138.0, 134.3, 127.5, 119.5, 118.9, 115.9 (q, J = 287.6 Hz), 85.3, 81.5, 72.2, 71.7, 42.5, 38.8, 33.0, 30.2, 29.4, 20.4, 20.2, 9.6. HRMS (FAB) m/z 690.1915 (MNa^+ [$C_{28}H_{32}F_3N_7O_7SNa$] = 690.1934).

Procedure G: General Method for Removal of Acetyl and Trifluoroacetyl Protecting Groups. Example: 5′-*S*-(2-Aminoethyl)-6-*N*-(4-nitrobenzyl)-5′-thioadenosine (3). A mixture of **25a** (100 mg, 0.16 mmol) in 30% NH_3/H_2O (1 mL) and MeOH (1 mL) was heated at 60 °C in a sealed pressure tube until deprotection was complete (~6 h, TLC). Volatiles were removed to give a residue containing one major TLC-visible product **3**. HRMS (FAB) m/z 462.1565 (MH^+ [$C_{19}H_{24}N_7O_5S$] = 462.1560). The residue was used directly in coupling reactions with FITC or **23**.

5′-*S*-(2-Aminoethyl)-6-*N*-[(4-propanamido)benzyl]-5′-thioadenosine (26b). Treatment of **25b** (63 mg, 0.094 mmol) by procedure G gave a residue containing **26b**. HRMS (FAB) m/z 510.1886 (MNa^+ [$C_{22}H_{29}N_7O_4SNa$] = 510.1899) that was used directly in coupling reactions with FITC or **23**.

6-(Trifluoroacetamido)hexanoic Acid (22). A mixture of 6-aminohexanoic acid (**21**) (3.32 g, 25.3 mmol) in trifluoroacetic anhydride (7 mL) was stirred for 1 h at ambient temperature and then for 3 h at 80 °C. Volatiles were removed under vacuum, and

the residue was dissolved in EtOAc. The solution was washed (H_2O), and volatiles were removed under vacuum. Recrystallization of the residue (EtOAc/Et_2O) gave **22** (4.16 g, 72%). ^{1}H NMR (DMSO-d_6, 500 MHz) δ 11.98 (s, 1H), 9.38 (s, 1H), 3.16 ("q", J = 6.7 Hz, 2H), 2.19 (t, J = 7.3 Hz, 2H), 1.44−1.53 (m, 4H), 1.23−1.29 (m, 2H). HRMS (EI) m/z 228.0836 (MH^+ [$C_8H_{13}F_3NO_3$] = 228.0848).

4-Nitrophenyl 6-(Trifluoroacetamido)hexanoate (23). A mixture of **22** (1.26 g, 5.55 mmol), 4-nitrophenol (930 mg, 6.69 mmol), and DCC (1.39 g, 6.73 mmol) in CH_2Cl_2 (10 mL) was stirred overnight at ambient temperature. DCU was filtered and volatiles were removed under vacuum. Flash chromatography of the residue (20 → 30% EtOAc/hexanes) gave **23** (1.73 g, 90%). ^{1}H NMR ($CDCl_3$, 500 MHz) δ 8.27 (d, J = 9.5 Hz, 2H), 7.28 (d, J = 9.0 Hz, 2H), 6.47 (br s, 1H), 3.41 ("q", J = 7.0 Hz, 2H), 2.63 (t, J = 7.3 Hz, 2H), 1.77−1.83 (m, 2H), 1.64−1.70 (m, 2H), 1.45−1.52 (m, 2H). HRMS (FAB) m/z 349.1021 (MH^+ [$C_{14}H_{16}F_3N_2O_5$] = 349.1011).

6-*N*-(4-Nitrobenzyl)-5′-*S*-{2-[6-(trifluoroacetamido)hexanamido]-ethyl}-5′-thioadenosine (27a). A mixture of crude **3** (~0.36 mmol calculated from its precursor **25a**), **23** (125 mg, 0.36 mmol), and Et_3N (61 μL, 44 mg, 0.44 mmol) in DMF (3 mL) was stirred overnight at ambient temperature and volatiles were evaporated under vacuum. Flash chromatography of the residue (5 → 10% MeOH/CH_2Cl_2) gave **27a** (110 mg, 47%): UV (MeOH) max 271 nm, min 232 nm. ^{1}H NMR (MeOH-d_4, 500 MHz) δ 8.25 (s, 1H), 8.21 (s, 1H), 8.11 (d, J = 9.0 Hz, 2H), 7.54 (d, J = 8.5 Hz, 2H), 5.98 (d, J = 4.5 Hz, 1H), 4.75 (t, J = 5.0 Hz, 1H), 4.30 (t, J = 4.8 Hz, 1H), 4.18 (dd, J = 5.5, 10.5 Hz, 1H), 3.28−3.31 (m, 2H), 3.22 (t, J = 7.0 Hz, 2H), 2.97 (dd, J = 5.3, 13.8 Hz, 1H), 2.91 (dd, J = 6.5, 14.0 Hz, 1H), 2.64 (dt, J = 3.0, 7.0 Hz, 2H), 2.13 (t, J = 7.5 Hz, 2H), 1.49−1.60 (m, 4H), 1.25−1.32 (m, 2H). ^{13}C NMR (MeOH-d_4, 125 MHz) δ 176.2, 159.6 (q, J = 36.7 Hz), 156.2, 154.1, 150.3, 148.7, 148.6, 141.3, 129.4, 124.7, 121.2, 117.7 (q, J = 286.1 Hz), 90.2, 85.9, 75.0, 74.2, 44.5, 40.7, 40.2, 37.0, 35.2, 33.2, 29.7, 27.5, 26.6. HRMS (FAB) m/z 693.2037 (MNa^+ [$C_{27}H_{33}F_3N_8O_7SNa$] = 693.2043).

6-*N*-[4-(Propanamido)benzyl]-5′-*S*-{2-[6-(trifluoroacetamido)-hexanamido]ethyl}-5′-thioadenosine (27b). A mixture of crude **26b** (~0.20 mmol calculated from its precursor **25b**), **23** (82 mg, 0.24 mmol), and Et_3N (33 μL, 24 mg, 0.24 mmol) in DMF (3 mL) was stirred overnight at ambient temperature and volatiles were evaporated under vacuum. Flash chromatography of the residue (5 → 10% MeOH/CH_2Cl_2) gave **27b** (130 mg, 96%): UV (MeOH) max 266 nm, min 255 nm. ^{1}H NMR (DMSO-d_6, 500 MHz) δ 9.78 (s, 1H), 9.38 (br s, 1H), 8.37 (s, 1H), 8.33 (br s, 1H), 8.22 (s, 1H), 7.87 (t, J = 5.8 Hz, 1H), 7.49 (d, J = 8.5 Hz, 2H), 7.25 (d, J = 9.0 Hz, 2H), 5.90 (d, J = 6.0 Hz, 1H), 5.49 (d, J = 6.5 Hz, 1H), 5.31 (d, J = 5.0 Hz, 1H), 4.73−4.75 (m, 1H), 4.64 (br s, 2H), 4.14 (dd, J = 4.5, 9.0 Hz, 1H), 4.00 (dt, J = 4.0, 6.5 Hz, 1H), 3.13−3.20 (m, 4H), 2.92 (dd, J = 5.8, 13.8 Hz, 1H), 2.83 (dd, J = 6.8, 13.8 Hz, 1H), 2.56 (dt, J = 2.0, 7.0 Hz, 2H), 2.28 (q, J = 7.5 Hz, 2H), 2.03 (t, J = 7.3 Hz, 2H), 1.43−1.50 (m, 4H), 1.18−1.23 (m, 2H), 1.05 (t, J = 7.5 Hz, 3H). ^{13}C NMR (DMSO-d_6, 125 MHz) δ 172.0, 171.8, 156.1 (q, J = 35.8 Hz), 154.4, 152.6, 148.8, 139.8, 137.9, 134.4, 127.5, 119.6, 118.9, 116.0 (q, J = 288.5 Hz), 87.4, 83.8, 72.63, 72.55, 45.7, 42.5, 38.5, 35.2, 33.9, 31.4, 29.4, 28.0, 25.8, 24.8, 9.6. HRMS (FAB) m/z 719.2557 (MNa^+ [$C_{30}H_{39}F_3N_8O_6SNa$] = 719.2563).

5′-*S*-{2-[(6-Amino)hexanamido]ethyl}-6-*N*-(4-nitrobenzyl)-5′-thioadenosine (28a). Treatment of **27a** (55 mg, 0.082 mmol) by procedure G gave a residue containing **28a**. HRMS (FAB) m/z 575.2394 (MH^+ [$C_{25}H_{35}N_8O_6S$]=575.2400) that was used directly for conjugation with FITC.

5′-*S*-{2-[(6-Amino)hexanamido]ethyl}-6-*N*-[(4-propanamido)-benzyl]-5′-thioadenosine (28b). Treatment of **27b** (60 mg, 0.086 mmol) by procedure G gave a residue containing **28b**. HRMS (FAB) m/z 623.2753 (MNa^+ [$C_{28}H_{40}N_8O_5SNa$] = 623.2740) that was used directly for conjugation with FITC.

Procedure H: General Method for Conjugation of FITC with the Pendant Amino Group at C5′. Example: 5a. A mixture of FITC (58 mg, 90% isomer I, 0.13 mmol), crude **3** (~0.13 mmol calculated from its precursor **25a**), and Et_3N (56 μL, 41 mg, 0.41 mmol) in DMF (2 mL) was stirred *with protection from light* for 3 h at ambient temperature and volatiles were removed under vacuum. Flash chromatography of the residue (10 → 12 → 15% MeOH/CH_2Cl_2) gave **5a** (64 mg, 56%): UV−vis (50 mM pH 7.0 phosphate buffer) max 241, 265, 367, 496 nm (ε 47 100, 39 100, 5200, 42 100), min 227, 255, 362, 409 nm (ε 38 400, 37 600, 4300, 2900). ^{1}H NMR (DMSO-d_6, 500 MHz) δ 10.15−10.21 (br m, 3H), 8.59 (br s, 1H), 8.44 (s, 1H), 8.26 (br s, 1H), 8.24 (s, 1H), 8.22 (s, 1H), 8.17 (d, J = 9.0 Hz, 2H), 7.74 (d, J = 8.0 Hz, 1H), 7.57 (d, J = 8.5 Hz, 2H), 7.17 (d, J = 8.0 Hz, 1H), 6.67 (d, J = 2.0 Hz, 2H), 6.55−6.61 (m, 4H), 5.92 (d, J = 5.5 Hz, 1H), 5.53 (d, J = 6.0 Hz, 1H), 5.38 (br s, 1H), 4.80 (br s, 3H), 4.18 (br s, 1H), 4.05−4.09 (m, 1H), 3.68−3.69 (br m, 2H), 3.01 (dd, J = 6.0, 14.0 Hz, 1H), 2.93 (dd, J = 6.8, 13.8 Hz, 1H), 2.74−2.80 (m, 2H). ^{13}C NMR (DMSO-d_6, 125 MHz) 180.4, 168.5, 159.8, 154.3, 152.6, 152.0, 149.0, 148.3, 146.8, 146.3, 141.2, 140.2, 129.4, 129.1, 128.0, 126.8, 124.2, 123.5, 119.7, 116.7, 112.7, 109.8, 102.2, 87.5, 84.0, 72.6, 43.5, 42.6, 33.8, 30.5. HRMS (FAB) m/z 851.1921 (MH^+ [$C_{40}H_{35}N_8O_{10}S_2$] = 851.1918).

5b: Treatment of a mixture of FITC (50 mg, 90% isomer I, 0.12 mmol), crude **26b** (~ 0.12 mmol calculated from its precursor **25b**), and Et_3N (48 μL, 35 mg, 0.35 mmol) in DMF by procedure H gave **5b** (96 mg, 95%; flash chromatography with 10 → 15 → 20% MeOH/CH_2Cl_2): UV−vis (50 mM pH 7.0 phosphate buffer) max 241, 264 (sh), 320 (sh), 367 (sh), 496 nm (ε 51 700, 40 100, 6500, 4200, 39 800), min 226, 406 nm (ε 39 800, 2900). ^{1}H NMR (DMSO-d_6, 500 MHz) δ 10.11 (br s, 2H), 10.05 (br s, 1H), 9.78 (s, 1H), 8.38 (s, 1H), 8.34 (br s, 1H), 8.22 (s, 2H), 8.15 (br s, 1H), 7.73 (d, J = 7.5 Hz, 1H), 7.49 (d, J = 9.0 Hz, 2H), 7.24 (d, J = 8.5 Hz, 2H), 7.17 (d, J = 8.0 Hz, 1H), 6.67 (d, J = 2.5 Hz, 2H), 6.55−6.61 (m, 4H), 5.91 (d, J = 6.0 Hz, 1H), 5.51 (d, J = 5.5 Hz, 1H), 5.33 (d, J = 5.0 Hz, 1H), 4.76−4.78 (m, 1H), 4.63 (br s, 2H), 4.16−4.18 (m, 1H), 4.04−4.08 (m, 1H), 3.69−3.70 (br m, 2H), 3.01 (dd, J = 6.0, 14.0 Hz, 1H), 2.92 (dd, J = 7.3, 13.8 Hz, 1H), 2.75−2.81 (m, 2H), 2.27 (q, J = 7.5 Hz, 2H), 1.05 (t, J = 7.5 Hz, 3H). ^{13}C NMR (DMSO-d_6, 125 MHz) δ 180.4, 171.8, 168.5, 159.6, 154.4, 152.6, 151.9, 148.8, 147.2, 141.2, 139.9, 138.0, 134.5, 129.6, 129.1, 127.5, 126.6, 124.1, 119.6, 118.9, 116.6, 112.6, 109.7, 102.2, 87.4, 83.9, 72.64, 72.62, 43.5, 42.5, 33.8, 30.5, 29.4, 9.7. HRMS (FAB) m/z 877.2430 (MH^+ [$C_{43}H_{41}N_8O_9S_2$] = 877.2438).

7a: Treatment of a mixture of FITC (33 mg, 90% isomer I, 0.077 mmol), crude **28a** (~ 0.078 mmol, calculated from its precursor **27a**), and Et_3N (33 μL, 24 mg, 0.24 mmol) in DMF by procedure H gave **7a** (64 mg, 86%; flash chromatography with 10 → 15 → 20% MeOH/CH_2Cl_2): UV−vis (50 mM pH 7.0 phosphate buffer) max 240, 265, 367, 496 nm (ε 53 700, 43 100, 7200, 47 500), min 227, 256, 362, 409 nm (ε 45 600, 42 000, 5800, 4000). ^{1}H NMR (DMSO-d_6, 500 MHz) δ 10.13 (br s, 2H), 10.04 (br s, 1H), 8.59 (br s, 1H), 8.43 (s, 1H), 8.27 (s, 1H), 8.22 (s, 1H), 8.16−8.18 (m, 3H), 7.91 (t, J = 5.8 Hz, 1H), 7.74 (d, J = 7.0 Hz, 1H), 7.58 (d, J = 8.5 Hz, 2H), 7.17 (d, J = 8.5 Hz, 1H), 6.67 (d, J = 2.5 Hz, 2H), 6.55−6.61 (m, 4H), 5.91 (d, J = 6.0 Hz, 1H), 5.52 (d, J = 6.5 Hz, 1H), 5.35 (d, J = 4.5 Hz, 1H), 4.81 (br s, 2H), 4.76−4.77 (br m, 1H), 4.14−4.15 (br m, 1H), 4.00−4.03 (m, 1H), 3.47−3.48 (br m, 2H), 3.17−3.21 (m, 2H), 2.93 (dd, J = 5.8, 13.8 Hz, 1H), 2.84 (dd, J = 6.8, 13.8 Hz, 1H), 2.56 (dt, J = 2.5, 7.0 Hz, 2H), 2.07 (t, J = 7.5 Hz, 2H), 1.49−1.58 (m, 4H), 1.26−1.32 (m, 2H). ^{13}C NMR (DMSO-d_6, 125 MHz) δ 180.3, 172.1, 168.6, 159.6, 154.3, 152.6, 151.9, 149.0, 148.3, 146.8, 146.3, 141.5, 140.2, 129.3, 129.1, 128.0, 126.6, 124.1, 123.5, 119.7, 116.3, 112.6, 109.8, 102.2, 87.4, 83.9, 72.64, 72.57, 43.7, 42.6, 38.5, 35.3, 33.9, 31.4, 28.2, 26.2, 25.0. HRMS (FAB) m/z 964.2756 (MH^+ [$C_{46}H_{46}N_9O_{11}S_2$] = 964.2758).

7b: Treatment of a mixture of FITC (36 mg, 90% isomer I, 0.082 mmol), crude **28b** (~0.081 mmol calculated from its

precursor **27b**), and Et_3N (34 μL, 25 mg, 0.25 mmol) in DMF by procedure H (flash chromatography with 15 → 20% MeOH/CH_2Cl_2) gave **7b** (71 mg, 89%): UV−vis (50 mM pH 7.0 phosphate buffer) max 240, 263 (sh), 318 (sh), 367, 496 nm (ε 37 800, 28 400, 4700, 3300, 33 300), min 226, 361, 410 nm (ε 30 700, 3000, 2100). ^{1}H NMR (DMSO-d_6, 500 MHz) δ 10.18 (br s, 2H), 10.07 (br s, 1H), 9.82 (s, 1H), 8.39 (br s, 2H), 8.27 (br s, 1H), 8.23 (br s, 2H), 7.93 (t, J = 5.8 Hz, 1H), 7.74 (d, J = 7.0 Hz, 1H), 7.49 (d, J = 8.5 Hz, 2H), 7.25 (d, J = 8.0 Hz, 2H), 7.17 (d, J = 8.5 Hz, 1H), 6.67 (d, J = 2.0 Hz, 2H), 6.55−6.62 (m, 4H), 5.90 (d, J = 5.5 Hz, 1H), 5.53 (d, J = 6.5 Hz, 1H), 5.37 (d, J = 5.0 Hz, 1H), 4.75−4.76 (m, 1H), 4.64 (br s, 2H), 4.13−4.15 (m, 1H), 4.01 (dt, J = 4.0, 6.3 Hz, 1H), 3.48−3.50 (br m, 2H), 3.16−3.21 (m, 2H), 2.93 (dd, J = 6.3, 13.8 Hz, 1H), 2.84 (dd, J = 7.0, 14.0 Hz, 1H), 2.57 (dt, J = 2.5, 7.0 Hz, 2H), 2.28 (q, J = 7.5 Hz, 2H), 2.07 (t, J = 7.3 Hz, 2H), 1.49−1.58 (m, 4H), 1.26−1.32 (m, 2H), 1.05 (t, J = 7.8 Hz, 3H). ^{13}C NMR (DMSO-d_6, 125 MHz) δ 180.3, 172.1, 171.8, 168.6, 159.5, 154.4, 152.7, 151.9, 148.8, 146.9, 141.5, 139.9, 138.0, 134.5, 129.3, 129.1, 127.5, 126.5, 124.1, 119.5, 119.0, 116.3, 112.6, 109.8, 102.2, 87.4, 83.8, 72.7, 72.6, 43.8, 42.5, 38.5, 35.3, 33.9, 31.4, 29.4, 28.2, 26.2, 25.0, 9.7. HRMS (FAB) m/z 990.3290 (MH^+ $[C_{49}H_{52}N_9O_{10}S_2]$ = 990.3279).

Nucleoside Transport General. NBMPR, mineral oil, and other chemicals were obtained from Sigma Chemical Company (Mississauga, ON). [^{3}H]Uridine and [^{3}H]NBMPR were from Moravek Biochemicals (Brea, CA). Tissue culture plates (96-well) were from VWR Scientific (Whitby, ON). Cell culture media and fetal bovine serum (FBS) were from Invitrogen (Burlington, ON). Ecolite was from ICN Pharmaceuticals (Montreal, PQ) and 550 silicone oil was from BC Bearings (Edmonton, AB). The Cell Titer 96 Aqueous One Solution cell proliferation assay kit was from Promega (Madison, WI). Fluorescent quantification beads (Quantum FITC MESF beads) were from Bangs Laboratories (Hornby, ON).

The human CCRF-CEM leukemia (hereafter termed CEM) cell line was obtained from William T. Beck (The University of Illinois at Chicago). The S49 mouse lymphoma, L1210 mouse leukemia, HL-60 human lymphoblastoid leukemia, HeLa human cervical adenocarcinoma, K562 human erythroleukemia, and BeWo human choriocarcinoma cells were obtained from the American Type Culture Collection (Manassas, VA). Cells were grown in RPMI 1640 medium supplemented with 10% fetal bovine serum as suspension (CEM, CEM-ARAC, S49, L1210, HL-60, and K562) or adherent (HeLa and BeWo) cultures. Cells were determined to be free of mycoplasma, maintained in the absence of antibiotics, incubated at 37 °C in a humidified atmosphere (5% CO_2), and subcultured at 2- to 4-day intervals to maintain active proliferation. Cell numbers were determined with a Coulter Z2 electronic particle counter equipped with a size analyzer (Beckman Coulter Canada, Mississauga, ON). All transport and binding assays were performed at ambient temperature in sodium buffer containing 144 mM NaCl, 20 mM Tris, 3 mM K_2HPO_4, and 5 mM glucose at pH 7.4. Phosphate-buffered saline (PBS) was 0.01 M phosphate buffer containing 138 mM NaCl and 27 mM KCl at pH 7.2.

Inhibition of hENT1-Mediated [^{3}H]Uridine Transport in *Saccharomyces cerevisiae* with 18a−18w. hENT1 cDNAs were inserted into the yeast expression vector pYPGE15, and the resulting plasmids were transformed into fui1::TRP1 (MATα, gal, ura3-52, trp1, lys2, ade2, hisd2000, Δfui::TRP1) and maintained as described.[36,37] Yeast containing pYPhENT1 were grown in CMM/GLU medium to A_{600} 0.5−1.2, washed twice with fresh medium, and resuspended to A_{600} 4.0. Transport assays were performed at ambient temperature in 96-well plates as described.[36,37] Briefly, 50 μL portions of yeast suspensions were added to 50 μL portions of 2× concentrated [^{3}H]uridine in 96-well plates. Because the initial rates of uridine transport into yeast cells producing recombinant ENTs persist for intervals of 30−40 min,[38] single time points at 20 min were used to estimate the initial transport rates. Yeast cells were collected on filter mats with a Micro96 cell harvester (Skatron Instruments, Lier, Norway) and rapidly washed with deionized water. Individual filter circles corresponding to the wells of the 96-well plates were removed from the filter mats with forceps and transferred to vials for scintillation counting. Yeast suspensions were first incubated for 15 min with NBMPR (or analogue) solutions (3 nM) to allow equilibration of the inhibitor with binding sites before addition of radiolabeled uridine. Uptake was measured for 20 min as described.[38]

Evaluation of 5a, 5b, 7a, and 7b as Inhibitors of [^{3}H]NBMPR Binding to Yeast Producing Recombinant hENT1 and to CEM Cells. The four title compounds were evaluated in yeast producing recombinant hENT1 as described above and in CEM cells (which possess endogenous hENT1) as inhibitors of binding of [^{3}H]NBMPR (5 nM) in the absence or presence of unlabeled NBMPR, **5a**, **5b**, **7a**, or **7b** (each at 500 nM). Yeast were grown in CMM/GLU medium to A_{600} 0.5−1.2, washed twice with fresh medium, and resuspended to A_{600} 4.0. Yeast suspensions were incubated at ambient temperature for 60 min with 5 nM [^{3}H]NBMPR in the absence (control) or presence of unlabeled NBMPR, **5a**, **5b**, **7a**, or **7b**. After incubation, yeast were collected on filter mats with a Micro96 cell hyarvester and processed for scintillation counting as described for transport experiments. CEM cells were washed free of media, and suspensions containing 10^6 cells in 100 μL of sodium buffer were incubated at ambient temperature for 60 min with [^{3}H]NBMPR in the absence or presence of unlabeled NBMPR or title compound. The mixtures were then spun through oil to remove unbound [^{3}H]NBMPR, and cell pellets were solubilized with 5% Triton X-100 and analyzed by liquid scintillation counting.

Analysis of Cell-Surface Binding of 5a, 5b, 7a, and 7b to CEM Cells by Flow Cytometry. CEM cells were washed free of growth medium, resuspended in buffer to a density of 2.5×10^5 cells/mL, and incubated at ambient temperature for 1 h with either no added compound (negative control) or 100 nM concentrations of the title compounds. Cells were then collected by centrifugation, washed twice with buffer, and analyzed for fluorescence by analytical flow cytometry.

Conjugate **7a** was selected for further specificity testing. CEM cells were treated for 1 h under three conditions: (1) no compound added (negative control), (2) addition of **7a** (100 nM), or (3) addition of [**7a** (100 nM) + NBMPR (10 μM)]. Cells were collected after 1 h by centrifugation, washed twice with buffer, and analyzed for fluorescence by analytical flow cytometry.

Inhibition of the Influx of [^{3}H]uridine into CEM Cells with 7a. Measurement of the time course for [^{3}H]uridine uptake was conducted in sodium buffer at ambient temperature. Briefly, exponentially growing cells were collected, washed once with PBS, and resuspended in sodium buffer (100 μL, 10^6 cells/tube). [^{3}H]Uridine (2 μM, 100 μL) was added (final concentration 1 μM) in the absence or presence of NBMPR (1 μM) or **7a** (1 μM) or excess uridine (1 mM). Transport was allowed to proceed during 0−30 s, and the mixture was then spun through oil. The cell pellet was solubilized with 5% Triton X-100 and analyzed by liquid scintillation counting.

Cells were pretreated with graded concentrations of **7a** (0−10 μM) for 10 min in the inhibition experiments. Pretreated cells (100 μL; 10^6 cells) were added to [^{3}H]uridine in buffer (100 μL, 2 μM), transport was allowed to proceed for 30 s, and the cells were spun down and processed as described.

Inhibition of [^{3}H]NBMPR binding to CEM cells with 7a. Washed CEM cells (10^6 cells/tube) in sodium buffer were incubated at ambient temperature for 1 h with [^{3}H]NBMPR (10 nM) in the absence (control) or presence of graded concentrations of **7a** (0−1000 nM). The cells were then centrifuged through oil and processed as described above to measure bound [^{3}H]NBMPR. Nonspecific binding was measured in the presence of excess unlabeled NBMPR (10 μM). Specific binding (total minus nonspecific) was used for all analyses.

Protection of CEM Cells from Gemcitabine Cytotoxicity with NBMPR and 7a. CEM cells were seeded in 96-well plates (5×10^3 cells/well), incubated at 37 °C in a humidified atmosphere (5% CO_2) for 24 h and then exposed to graded concentrations of gemcitabine (0−100 μM) for 72 h in the absence or presence of NBMPR (1 μM) or **7a** (1 μM). After 72 h, the cells were treated with MTS reagent and staining was measured. The concentration of drug that inhibited the growth of treated cells by 50% relative to that of untreated cells (IC_{50}) was calculated by nonlinear regression analysis of data plotted as percentages of control values against the logarithm of drug concentrations using Graph Pad Prism software, Version 4.0 (San Diego, CA).

Analysis of Cell-Surface Binding of 7a to Cultured Cells by Flow Cytometry. Cell-surface abundances of hENT1/SLC29A1 on cultured cells were determined with **7a**. Cells were washed free of growth media, resuspended in sodium buffer (with a final density of 2.5×10^5 cells/mL), and incubated at ambient temperature with no compound (control), **7a** (100 nM), or [**7a** (100 nM) + NBMPR (10 μM)]. After 1 h, cells were spun down, washed twice with buffer and analyzed for fluorescence by analytical flow cytometry. Fluorescence-standard beads with defined numbers of fluorescein molecules were treated under the same conditions used for the cells. MESF values were calculated after each experiment to convert **7a** binding to MESF for quantification of hENT1 sites.

Cell-Surface Staining and Confocal Microscopic Visualization of hENT1 Sites on *Saccharomyces cerevisiae*, *Xenopus laevis* Oocytes, and CEM Cells with 7a. Cell-surface abundances of hENT1 on yeast, oocytes, and CEM cells were determined with **7a**. Briefly, yeast, oocytes, or CEM cells were washed free of media, suspended in PBS (10^5 cells/mL), and incubated at ambient temperature with **7a** (0 or 100 nM) or [**7a** (100 nM) + NBMPR (10 μM)] in buffer for 1 h (for the latter experiment, cells were preincubated with NBMPR for 10 min prior to addition of **7a**), spun down, washed (once quickly), and a small volume of PBS was added. The cells were then seeded onto poly-L-lysine coated dishes and visualized with a Zeiss axioscope confocal microscope.

Acknowledgment. We thank Brigham Young University for three R. K. Robins, J. S. Bradshaw, and BYU Cancer Research Center Graduate Research Fellowships (Y.P.), pharmaceutical company unrestricted gift funds (M.J.R.), and the Canadian Institutes of Health Research (C.E.C., J.D.Y.). We thank the Cell Imaging Facility of the Cross Cancer Institute for providing help with confocal microscopy.

Supporting Information Available: Inhibition of [^{3}H]uridine transport by **18a−18w**; synthesis and characterization data for **13a−13j**, **16k−16t**, and some intermediates without numbers. This material is available free of charge via the Internet at http://pubs.acs.org.

References

(1) King, A. E.; Ackley, M. A.; Cass, C. E.; Young, J. D.; Baldwin, S. A. Nucleoside Transporters: From Scavengers to Novel Therapeutic Targets. *Trends Pharmacol. Sci.* **2006**, *27*, 416–425.
(2) Zhang, J.; Visser, F.; King, K. M.; Baldwin, S. A.; Young, J. D.; Cass, C. E. The Role of Nucleoside Transporters in Cancer Chemotherapy with Nucleoside Drugs. *Cancer Metastasis Rev.* **2007**, *26*, 85–110.
(3) Young, J. D.; Yao, S. Y.; Sun, L.; Cass, C. E.; Baldwin, S. A. Human Equilibrative Nucleoside Transporter (ENT) Family of Nucleoside and Nucleobase Transporter Proteins. *Xenobiotica* **2008**, *38*, 995–1021.
(4) Damaraju, V. L.; Sawyer, M. B.; Mackey, J. R.; Young, J. D.; Cass, C. E. Human Nucleoside Transporters: Biomarkers for Response to Nucleoside Drugs. *Nucleosides, Nucleotides Nucleic Acids* **2009**, *28*, 450–463.
(5) Wiley, J. S.; Taupin, J.; Jamieson, G. P.; Snook, M.; Sawyer, W. H.; Finch, L. R. Cytosine Arabinoside Transport and Metabolism in Acute Leukemias and T Cell Lymphoblastic Lymphoma. *J. Clin. Invest.* **1985**, *75*, 632–642.
(6) Cass, C. E.; King, K. M.; Montano, J. T.; Janowska-Wieczorek, A. A Comparison of the Abilities of Nitrobenzylthioinosine, Dilazep, and Dipyridamole to Protect Human Hematopoietic Cells from 7-Deazaadenosine (Tubercidin). *Cancer Res.* **1992**, *52*, 5879–5886.
(7) Gati, W. P.; Paterson, A. R.; Tyrrell, D. L.; Cass, C. E.; Moravek, J.; Robins, M. J. Nucleobase Transporter-Mediated Permeation of 2′,3′-Dideoxyguanosine in Human Erythrocytes and Human T-Lymphoblastoid CCRF-CEM Cells. *J. Biol. Chem.* **1992**, *267*, 22272–22276.
(8) Mackey, J. R.; Mani, R. S.; Selner, M.; Mowles, D.; Young, J. D.; Belt, J. A.; Crawford, C. R.; Cass, C. E. Functional Nucleoside Transporters Are Required for Gemcitabine Influx and Manifestation of Toxicity in Cancer Cell Lines. *Cancer Res.* **1998**, *58*, 4349–4357.
(9) Gati, W. P.; Larratt, L. M.; Turner, A. R. Cellular Abundance of es Nucleoside Transporters and Differential Drug Toxicity in Myelodysplastic Syndrome (MDS) Bone Marrow Cell Subpopulations. *Proc. West. Pharmacol. Soc.* **2001**, *44*, 93–96.
(10) Spratlin, J.; Sangha, R.; Glubrecht, D.; Dabbagh, L.; Young, J. D.; Dumontet, C.; Cass, C.; Lai, R.; Mackey, J. R. The Absence of Human Equilibrative Nucleoside Transporter 1 Is Associated with Reduced Survival in Patients with Gemcitabine-Treated Pancreas Adenocarcinoma. *Clin. Cancer Res.* **2004**, *10*, 6956–6961.
(11) Farrell, J. J.; Elsaleh, H.; Garcia, M.; Lai, R.; Ammar, A.; Regine, W. F.; Abrams, R.; Benson, A. B.; Macdonald, J.; Cass, C. E.; Dicker, A. P.; Mackey, J. R. Human Equilibrative Nucleoside Transporter 1 Levels Predict Response to Gemcitabine in Patients with Pancreatic Cancer. *Gastroenterology* **2009**, *136*, 187–195.
(12) Marechal, R.; Mackey, J. R.; Lai, R.; Demetter, P.; Peeters, M.; Polus, M.; Cass, C. E.; Young, J.; Salmon, I.; Deviere, J.; Van Laethem, J.-L. Human Equilibrative Nucleoside Transporter 1 and Human Concentrative Nucleoside Transporter 3 Predict Survival After Adjuvant Gemcitabine Therapy in Resected Pancreatic Adenocarcinoma. *Clin. Cancer Res.* **2009**, *15*, 2913–2919.
(13) Jennings, L. L.; Hao, C.; Cabrita, M. A.; Vickers, M. F.; Baldwin, S. A.; Young, J. D.; Cass, C. E. Distinct Regional Distribution of Human Equilibrative Nucleoside Transporter Proteins 1 and 2 (hENT1 and hENT2) in the Central Nervous System. *Neuropharmacology* **2001**, *40*, 722–731.
(14) Wiley, J. S.; Snook, M. B.; Jamieson, G. P. Nucleoside Transport in Acute Leukaemia and Lymphoma: Close Relation to Proliferative Rate. *Br. J. Haematol.* **1989**, *71*, 203–207.
(15) Wiley, J. S.; Brocklebank, A. M.; Snook, M. B.; Jamieson, G. P.; Sawyer, W. H.; Craik, J. D.; Cass, C. E.; Robins, M. J.; McAdam, D. P.; Paterson, A. R. A New Fluorescent Probe for the Equilibrative Inhibitor-Sensitive Nucleoside Transporter. 5′-*S*-(2-Aminoethyl)-N^6-(4-nitrobenzyl)-5′-thioadenosine (SAENTA)-χ_2-fluorescein. *Biochem. J.* **1991**, *273*, 667–672.
(16) Jamieson, G. P.; Brocklebank, A. M.; Snook, M. B.; Sawyer, W. H.; Buolamwini, J. K.; Paterson, A. R.; Wiley, J. S. Flow Cytometric Quantitation of Nucleoside Transporter Sites on Human Leukemic Cells. *Cytometry* **1993**, *14*, 32–38.
(17) Wiley, J. S.; Cebon, J. S.; Jamieson, G. P.; Szer, J.; Gibson, J.; Woodruff, R. K.; McKendrick, J. J.; Sheridan, W. P.; Biggs, J. C.; Snook, M. B.; Brocklebank, A. M.; Rallings, M. C.; Paterson, A. R. P. Assessment of Proliferative Responses to Granulocyte-Macrophage Colony-Stimulating Factor (GM-CSF) in Acute Myeloid Leukaemia Using a Fluorescent Ligand for the Nucleoside Transporter. *Leukemia* **1994**, *8*, 181–185.
(18) Gati, W. P.; Paterson, A. R.; Larratt, L. M.; Turner, A. R.; Belch, A. R. Sensitivity of Acute Leukemia Cells to Cytarabine Is a Correlate of Cellular es Nucleoside Transporter Site Content Measured by Flow Cytometry with SAENTA-fluorescein. *Blood* **1997**, *90*, 346–353.
(19) Sen, R. P.; Delicado, E. G.; Alvarez, A.; Brocklebank, A. M.; Wiley, J. S.; Miras-Portugal, M. T. Flow Cytometric Studies of Nucleoside Transport Regulation in Single Chromaffin Cells. *FEBS Lett.* **1998**, *422*, 368–372.
(20) Paul, B.; Chen, M. F.; Paterson, A. R. P. Inhibitors of Nucleoside Transport. Structure−Activity Study Using Human Erythrocytes. *J. Med. Chem.* **1975**, *18*, 968–973.
(21) Fleming, S. A.; Rawlins, D. B.; Samano, V.; Robins, M. J. Photochemistry of Nucleoside Transport Inhibitor 6-*S*-Benzylated Thiopurine Ribonucleosides. Implications for a New Class of Photoaffinity Labels. *J. Org. Chem.* **1992**, *57*, 5968–5976.
(22) Agbanyo, F. R.; Vijayalakshmi, D.; Craik, J. D.; Gati, W. P.; McAdam, D. P.; Asakura, J.; Robins, M. J.; Paterson, A. R. P.; Cass, C. E. 5′-*S*-(2-Aminoethyl)-N^6-(4-nitrobenzyl)-5′-thioadenosine (SAENTA), a Novel Ligand with High Affinity for Polypeptides Associated with Nucleoside Transport. Partial Purification

of the Nitrobenzylthioinosine-Binding Protein of Pig Erythrocytes by Affinity Chromatography. *Biochem. J.* **1990**, *270*, 605–614.
(23) Buolamwini, J. K.; Craik, J. D.; Wiley, J. S.; Robins, M. J.; Gati, W. P.; Cass, C. E.; Paterson, A. R. P. Conjugates of Fluorescein and SAENTA [5′-*S*-(2-Aminoethyl)-N^6-(4-nitrobenzyl)-5′-thioadenosine]: Flow Cytometry Probes for the *ES* Nucleoside Transporter Elements of the Plasma Membrane. *Nucleosides Nucleotides* **1994**, *13*, 737–751.
(24) Robins, M. J.; Asakura, J.; Kaneko, M.; Shibuya, S.; Jacobs, E. S.; Agbanyo, F. R.; Cass, C. E.; Paterson, A. R. P. Synthesis of Substituted-Benzyl and Sugar-Modified Analogs of 6-*N*-(4-Nitrobenzyl)adenosine and Their Interactions with "*ES*" Nucleoside Transport Systems. *Nucleosides Nucleotides* **1994**, *13*, 1627–1646.
(25) Robins, M. J.; Uznański, B. Nucleic Acid Related Compounds. 34. Nonaqueous Diazotization with *tert*-Butyl Nitrite. Introduction of Fluorine, Chlorine, and Bromine at C-2 of Purine Nucleosides. *Can. J. Chem.* **1981**, *59*, 2608–2611.
(26) Liu, J.; Robins, M. J. Fluoro, Alkylsulfanyl, and Alkylsulfonyl Leaving Groups in Suzuki Cross-Coupling Reactions of Purine 2′-Deoxynucleosides and Nucleosides. *Org. Lett.* **2005**, *7*, 1149–1151.
(27) Liu, J.; Robins, M. J. S_NAr Displacements with 6-(Fluoro, Chloro, Bromo, Iodo, and Alkylsulfonyl)purine Nucleosides: Synthesis, Kinetics, and Mechanism. *J. Am. Chem. Soc.* **2007**, *129*, 5962–5968.
(28) Robins, M. J.; Hansske, F.; Wnuk, S. F.; Kanai, T. Nucleic Acid Related Compounds. 66. Improved Syntheses of 5′-Chloro-5′-deoxy- and 5′-S-Aryl(or Alkyl)-5′-thionucleosides. *Can. J. Chem.* **1991**, *69*, 1468–1474.
(29) Mani, R. S.; Hammond, J. R.; Marjan, J. M. J.; Graham, K. M.; Young, J. D.; Baldwin, S. A.; Cass, C. E. Demonstration of Equilibrative Nucleoside Transporters (hENT1, hENT2) in Nuclear Envelopes of Cultured Human Choriocarcinoma (BeWo) Cells by Functional Reconstitution in Proteoliposomes. *J. Biol. Chem.* **1998**, *273*, 30818–30825.
(30) Crawford, C. R.; Ng, C. Y.; Ullman, B.; Belt, J. A. Identification and Reconstitution of the Nucleoside Transporter of CEM Human Leukemia Cells. *Biochim. Biophys. Acta* **1990**, *1024*, 289–297.
(31) Paproski, R. J.; Ng, A. M. L.; Yao, S. Y. M.; Graham, K.; Peng, Y.; Robins, M. J.; Young, J. D.; Cass, C. E. The Role of Human Nucleoside Transporters in Uptake of 3′-Deoxy-3′-fluorothymidine. *Mol. Pharmacol.* **2008**, *74*, 1372–1380.
(32) Paproski, R. J.; Young, J. D.; Cass, C. E. Predicting Gemcitabine Transport and Toxicity in Human Pancreatic Cancer Cell Lines with the Positron Emission Tomography Tracer 3′-Deoxy-3′-fluorothymidine. *Biochem. Pharmacol.* **2010**, *79*, 587–595.
(33) Visser, F.; Sun, L.; Damaraju, V.; Tackaberry, T.; Peng, Y.; Robins, M. J.; Baldwin, S. A.; Young, J. D.; Cass, C. E. Residues 334 and 338 in Transmembrane Segment 8 of Human Equilibrative Nucleoside Transporter 1 Are Important Determinants of Inhibitor Sensitivity, Protein Folding, and Catalytic Turnover. *J. Biol. Chem.* **2007**, *282*, 14148–14157.
(34) Cai, J.; Damaraju, V. L.; Groulx, N.; Mowles, D.; Peng, Y.; Robins, M. J.; Cass, C. E.; Gros, P. Two Distinct Molecular Mechanisms Underlying Cytarabine Resistance in Human Leukemic Cells. *Cancer Res.* **2008**, *68*, 2349–2357.
(35) Robins, M. J.; Sarker, S.; Wnuk, S. F. What Are the Practical Limits for Detection of Minor Nucleoside Reaction Products with HPLC (UV Detection), ^{1}H NMR, and TLC (UV Detection)? *Nucleosides Nucleotides* **1998**, *17*, 785–790.
(36) Zhang, J.; Visser, F.; Vickers, M. F.; Lang, T.; Robins, M. J.; Nielsen, L. P. C.; Nowak, I.; Baldwin, S. A.; Young, J. D.; Cass, C. E. Uridine Binding Motifs of Human Concentrative Nucleoside Transporters 1 and 3 Produced in Saccharomyces Cerevisiae. *Mol. Pharmacol.* **2003**, *64*, 1512–1520.
(37) Vickers, M. F.; Zhang, J.; Visser, F.; Tackaberry, T.; Robins, M. J.; Nielsen, L. P. C.; Nowak, I.; Baldwin, S. A.; Young, J. D.; Cass, C. E. Uridine Recognition Motifs of Human Equilibrative Nucleoside Transporters 1 and 2 Produced in *Saccharomyces Cerevisiae*. *Nucleosides Nucleotides Nucleic Acids* **2004**, *23*, 361–373.
(38) Vickers, M. F.; Kumar, R.; Visser, F.; Zhang, J.; Charania, J.; Raborn, R. T.; Baldwin, S. A.; Young, J. D.; Cass, C. E. Comparison of the Interaction of Uridine, Cytidine, and Other Pyrimidine Nucleoside Analogues with Recombinant Human Equilibrative Nucleoside Transporter 2 (hENT2) Produced in Saccharomyces Cerevisiae. *Biochem. Cell Biol.* **2002**, *80*, 639–644.